Altered subcutaneous adipose tissue parameters after switching ART-controlled HIV+ patients to raltegravir/maraviroc

Jean-Philippe Bastard, Véronique Pelloux, Rohia Alili, Soraya Fellahi, Judith Aron-Wisnewsky, Emilie Capel, Bruno Fève, Lambert Assoumou, Edi Prifti, Christine Katlama, et al.

Altered subcutaneous adipose tissue parameters after switching ART-controlled HIV+ patients to raltegravir/maraviroc

Jean-Philippe BASTARD[1,2], Véronique PELLOUX[3,4], Rohia ALILI[3,4], Soraya FELLAHI[1], Judith ARON-WISNEWSKY[3,4], Emilie CAPEL[1], Bruno FÈVE[1,5], Lambert ASSOUMOU[6], Edi PRIFTI[7], Christine KATLAMA[6,8], Karine CLÉMENT[3,4], Jacqueline CAPEAU[1]

[1]Sorbonne Université, Inserm, Faculty of Medicine, Centre de Recherche Saint-Antoine (CRSA), ICAN, Paris, France

[2]Department of Biochemistry-Pharmacology-Molecular Biology, APHP, Henri-Mondor Hospital, Université Paris Est Créteil, France

[3] Sorbonne Université, Inserm, Faculty of Medicine, Nutrition and obesities: systemic approaches (NutriOmics), Paris, France

[4] Assistance Publique Hôpitaux de Paris, Sorbonne Université, Nutrition department, Pitié-Salpétrière hospital, CRNH Ile-de-France, GH APHP-Sorbonne Université, Paris, France

[5]Department of Endocrinology, CRMR Prisis, Saint-Antoine Hospital, GH APHP-Sorbonne Université, Paris France

[6] Sorbonne Université, Inserm, Faculty of Medicine, Institut Pierre Louis d'Epidémiologie et de Santé Publique (IPLESP), Paris, France

[7]IRD, Sorbonne University, UMMISCO, Bondy, France

[8]Department of Infectious Diseases, Pitié-Salpétrière hospital, GH APHP-Sorbonne Université, Paris France

Short title: fat alterations induced by RAL/MVC

Corresponding author and author to whom requests for reprints should be made:

Pr Jacqueline Capeau

Faculty of Medicine Sorbonne University, 27 rue Chaligny 75012 Paris France

e-mail: jacqueline.capeau@inserm.fr

Conflict of interest and source of funding

BF has received personal fees for lectures from Amgen, Sanofi, Lilly, Astra-Zeneca, Novo Nordisk

JC has received grants from ViiV healthcare and MSD, and personal fees for lectures from ViiV healthcare, MSD, Gilead, Janssen.

For the remaining authors none were declared

The ANRS 157 ROCnRAL study was sponsored and funded by the French National Institute for Health and Medical Research (INSERM)–French National Agency for Research on AIDS and Viral Hepatitis (ANRS); ViiV Healthcare (France) and Merck Sharp & Dohme (France) provided maraviroc and raltegravir, respectively, for this trial.

This study received a grant from ANRS. Support was also obtained by RHU CARMMA grant (ANR-15-RHUS-0003), the French National Agency of Research (ANR-Captor project), and ANR-10-IAHU-05 (IHU-ICAN) and FORCE (as part of F-Crin), as well as the Fondation pour la Recherche Médicale (FRM DEQ20120323701 and EQU201903007868).

Abstract

Objective: To evaluate the effect on anthropometric, metabolic and adipose tissue parameters of switching ART-controlled persons living with HIV (PLWH) from a protease-inhibitor regimen to raltegravir/maraviroc.

Design: Substudy of ROCnRAL-ANRS157 with investigation of subcutaneous abdominal adipose tissue (SCAT) biopsy at inclusion and study end.

Methods: We performed lipoaspiration of paired SCAT samples, histology on fresh/fixed samples and examined the transcriptomic profile analyzed using Illumina microarrays after RNA extraction. Statistical analyses used Wilcoxon-paired test.

Results: The patients (n=8) were mainly male (7/8), aged (mean±SEM) 54.9±1.2 years, BMI 26.1±1.2 kg/m^2, CD4: 699±56 cells/mm^3, all viral load (VL)<50 copies/mL. After a follow-up of 6±0.5 months, all PLWH remained with VL<50 copies/mL. BMI, trunk and limb fat amounts were unchanged yet systemic insulin resistance increased. Adipose tissue histology was unchanged except for borderline increased adipocyte diameter (*P*=0.1). Amongst the 16,094 RNA transcripts, 458 genes were up-regulated and 244 down-regulated. Analyses of the KEGG and GO databases, evaluating modifications in the main functional pathways, revealed that genes related to immune recognition/function were less expressed as were genes encoding T-cell receptor and receptor signaling pathways. The gene expression profiles indicated decreased

inflammation but genes involved in adipogenesis and insulin resistance were overexpressed.

Conclusion: After 6 months of raltegravir/maraviroc, adipogenesis-related gene profile was enhanced in SCAT, in agreement with a tendency for increased adipocyte size. Enhanced SCAT insulin resistance-related profile was concordant with higher systemic insulin resistance. However, immune activation/inflammation profile was globally lowered. We propose that raltegravir/maraviroc might favor SCAT gain but reduce inflammation/immune activation.

Key words

Subcutaneous adipose tissue, raltegravir, maraviroc, transcriptomics, histology, adipogenesis, inflammation/immune activation, insulin resistance

Introduction

Integrase strand transfer inhibitors (INSTI) are currently a highly recommended option in ART-naïve and also ART-experienced people living with HIV(PLWH) given their high and rapid efficacy and safe metabolic profile. However, some INSTIs (mainly dolutegravir and bictegravir but also raltegravir) have been recently associated with a global weight and fat mass gain[1]. Even if the mechanisms remain elusive, we have previously shown that some INSTIs induced adipocyte hypertrophy, adipose tissue (AT) fibrosis and insulin resistance[2]. However, in this previous work evaluating PLWH with severe obesity, we could only cross-compare AT samples issued from INSTI-treated or INSTI-untreated PLWH. The ROCnRAL study (Clinical-Trials.gov: NCT1420523), evaluated the efficacy of a dual therapy associating an INSTI, raltegravir, to the CCR5 inhibitor, maraviroc, in patients suppressed on a protease-inhibitor (PI)-containing regimen but was prematurely stopped due to insufficient virologic control[3]. Herein, we analyzed SCAT individual variation before and 6 months after raltegravir/maraviroc initiation.

Increased weight/fat has been reported in PLWH who received some PI-based treatment[1]. Due to PI-related increased risk of cardiometabolic diseases, aging PLWH have been often switched to an INSTI-based therapy due to the lipid-lowering effect of INSTI[4-6]. However, INSTI-related weight/fat gain also raises concern regarding increased cardiometabolic risk. This risk has not been yet clearly shown for cardiovascular diseases. Regarding insulin resistance and diabetes, results are discrepant[4, 7].

Otherwise, maraviroc has been associated with changes in immune profile and a favorable effect on cardiovascular parameters in PLWH[8, 9]. Moreover, maraviroc may exert anti-fibrotic effects on the liver[10, 11].

We performed a careful investigation of patients from the ROCnRAL study and examined the individual evolution of anthropometric, metabolic, inflammatory and AT parameters six months after initiation of the dual raltegravir/maraviroc therapy.

Patients and methods

Patients

Seventeen patients were enrolled into the ROCnRAL fat sub-study prior to study discontinuation. Eight had subcutaneous-AT (SCAT) biopsies both at initiation and end: they were aged (mean±SEM) 54.9±1.2 years at inclusion, 87% male, 87% Caucasian, 13% African, CD4 699±56 cells/mm^3, VL<50 copies/mL. They received raltegravir/maraviroc for a mean duration of 6±0.5 months.

Systemic markers

Adiponectin, leptin and inflammatory markers (hsCRP, hsIL-6, sCD14, sCD163) were measured on stored serum samples by immunonephelometry or ELISA[12]. Insulin resistance was measured by the quantitative insulin sensitivity check index (QUICKI) = $1/[\log(G_b) + \log(I_b)]$ where G_b is fasting plasma glucose (milligrams per deciliter), and I_b is fasting plasma insulin (microunits per milliliter).

Fat collection and histology

Subcutaneous-AT(SCAT) samples were collected by a single operator (JPB) by needle lipoaspiration from the periumbilical area under local anesthesia.

Histology was analyzed on fresh tissue to evaluate adipocyte size/volume and on fixed tissue to evaluate fibrosis by Sirius Red staining (scored using arbitrary units 0-3)[13].

mRNA extraction and transcriptomics

Total RNA was extracted using a RNeasy total-RNA minikit (QIAGEN, Verlo, The Netherlands), quality/concentration assessed (Agilent-2100 bioanalyzer, Agilent-Technologies, Santa-Clara, USA) and biotin-labeled complementary-RNA obtained (Ambion, Thermo-Fischer-Scientific, Waltham, USA). Hybridization processes used Illumina human HT-12 version-4.0 Expression BeadChips (Illumina-Inc, San-Diego, USA). Probes were detected using an Illumina-BeadArray Reader[14].

Raw data were extracted using the numerical results (Illumina Genome-Studio 2011.1 software). The group comparisons used Student's *t* test. To estimate the false-discovery-rate, we filtered the resulting *P* values at 5% and used the Benjamini-Hochberg procedure[14]. In the 16 paired samples, 80% of genes had valid expression. The Significance Analysis of Microarrays (SAM), shown as a switch R plot, indicated the genes significantly up- and down-regulated after the switch (suppl Figure 1). An automated annotation procedure of the differentially expressed genes used the KEGG (Kyoto Encyclopedia of Genes and Genomes) or GO (Gene Ontology) annotation databases. Functional analyses used the FunNet package.

Statistics

The paired results were compared using Wilcoxon-test (significant *P*<5%, Prism and Statview software). Transcriptomics results were adjusted for multiple testing (significant q<5%, SAM package).

Results

All patients remained controlled (VL<50 copies/mL) with unmodified CD4 and CD8 levels (Table 1). BMI was unchanged after 6 months, as waist circumference, waist-to-hip ratio, trunk and limb fat amounts. However, hip circumference increased from 94.9 to 99.1 cm (*P*=0.03). Regarding metabolic parameters, insulin increased (10.7 to 21.5 mU/L, p<0.05). To evaluate insulin resistance, we used QUICKI, better correlated to the gold standard euglycemic hyper-insulinemic clamp IS value than HOMA-IR[15]: QUICKY decreased from 0.342 to 0.315 (*P*<0.05), in favor of increased insulin resistance. The level of adiponectin and inflammatory/immune activation markers (hsCRP, hsIL-6, sCD14, sCD163) was unmodified but leptin tended to increase (*P*=0.08, Table 1).

Adipose tissue histology revealed that adipocyte diameter and volume increased yet not reaching significance (*P* =0.10). The level of parenchyma fibrosis remained unchanged.

Transcriptomic analysis performed in the 16 paired samples identified 16,094 expressed RNA transcripts: 244 genes were down-regulated with a fold-change of 0.66 to 0.9 and 458 genes up-regulated with a fold-change of 10.6 to 1.1 (supplemental Tables 1 and 2).

Using the GO database, the gene network (Fig 1) revealed globally increased DNA replication and transcription, suggesting AT remodeling. Importantly, T-cell receptor signaling pathway was down-regulated as were pathways related to viral infection. Using the KEGG annotation database (Suppl Fig 2), the most enriched function was ubiquitin-mediated proteolysis (19.4%) and the main impoverished function (29.7%) was related to ribosomes involved in protein synthesis, indicating major switch-induced protein remodeling. Functions related to immune cell recognition and immune-related diseases were down-regulated.

Among the individual down- and up-regulated genes, we selected those with the larger amplitude of variation (less than x0.8 or more than x3). Two main categories were affected: *i)* genes expressed in immune cells and involved into T-cell and macrophage activation, and *ii)* genes involved into adipogenesis and insulin sensitivity in adipocytes. Among down-regulated immune-related genes, several encode proteins from the TCR superfamily: CD247 x0.7, TNFRSF4 (tumor-necrosis-factor receptor superfamily member-4) x0.7, CD3D (CD3 moleculeδ in the CD3-TCR complex) x0.7. Other genes encode proteins expressed in T-cells: IL7R x0.7 and GIMAP4 (GTPase, IMAP-family-member-4) x0.7 in the IL7R pathway, GZMB (granzyme B) x0.7, CD58 x0.8, SEMA4D (semaphoring-4D) x0.8, in favor of a decreased level of T-lymphocytes within AT.

Several immune-related genes were upregulated as genes expressed in macrophages favoring the M2 versus M1 phenotype: DAB2/CD11b x4.7, FOXO3 (forkhead-box-O3) x3.9, TCF4 (transcription factor-4) x3.6, CREB1 (cAMP-responsive-element-binding-protein-1) x3.5, IL10 x3.1. A number of genes were involved into decreased T-

lymphocyte immune activation: MAGT1 (magnesium transporter-1) x5.3, DAB2/CD11b x4.7, IL17RD (IL17 receptor-D) x4.0. Also, genes encoding proteins inhibiting NFκB and decreasing inflammation were up-regulated: CDKN2AIPNL (CDKN2A-interacting-protein-N-terminal-like) x7.7, DUSP19 (dual-specificity phosphatase-19) x5.6, KLF6 (Kruppel-like factor-6) x5.5, TRIM3 (tripartite-motif-containing-13) x3.3, while few genes were positively involved into inflammation as SEMA3E (semaphoring-3E) x4.9. Taken as a whole, the gene expression profile suggested decreased T-lymphocytes number/activation and a shift to a M2 macrophage phenotype together with increased expression of anti-inflammatory genes.

Otherwise, up-regulated expression was observed for genes involved into adipogenesis: KLF6 x5.5, QRFRR (polyglutamated RF-amide peptide receptor) x5.5, CREB1 x5.0, FOXO3 x3.9, TRIM13 x3.3, DLC1 (deleted-in-liver-cancer-1) x3.3, IL10 x3.1.

Also, several genes in the insulin signaling pathways involved into increased insulin resistance were up-regulated: SEMA3E x4.9, PIP5K2B (phosphatidylinositol-5-phosphate-4-kinase, typeIIβ) x3.7, IL10 x3.1, while LEPROT (leptin-receptor-overlapping-transcript) x5.4 is related to insulin signaling.

Discussion

We report here that ART-suppressed PLWH switched to raltegravir/maraviroc presented metabolic and adipose tissue modifications over six months. While BMI and fat mass did not change, hip circumference increased indicating fat redistribution. Likewise, insulin resistance, evaluated by fasting glycemia/insulin levels, increased. SCAT exhibited enhanced expression of genes associated with adipogenesis and insulin resistance.

Otherwise, expression of genes related to T-lymphocytes was reduced and the gene profile suggested a shift towards decreased AT inflammation and a M2 anti-inflammatory macrophage phenotype.

INSTI have been recently associated with a global fat mass gain. We previously reported increased adipogenesis induced by dolutegravir and raltegravir *in vitro* together with adipocyte hypertrophy in SCAT and visceral AT samples issued from INSTI-treated PLWH and macaques[2]. Our present results are in good accordance. The fact that the two main categories of modified genes are involved into protein degradation/synthesis enlightens the marked effect of ART *versus* HIV on fat. Indeed, only switching ART regimen, without CD4 or VL change, deeply affected AT. Previous *in vitro* studies indicated that maraviroc was neutral regarding adipocyte differentiation[16]. Thus, increased adipogenesis, suggested by the gene expression profile, and borderline increased adipocyte size might result from the effect of raltegravir.

Regarding inflammation, in accordance with our present results, we observed in SCAT samples from obese PLWH the absence of inflammation (macrophage infiltration with crown-like structures) in samples issued from INSTI-treated patients by contrast to non-INSTI PLWH and HIV-negative controls[17]. Interestingly, increased weight in INSTI-treated PLWH was associated with decreased VAT density suggesting a lower inflammation level[18]. Therefore, INSTI could reduce AT inflammation and immune activation. Maraviroc was previously shown to decrease inflammatory cytokine expression in cultured adipocytes[16] and macrophage recruitment in AT induced by a

high-fat diet in mice[19]. Thus, both raltegravir and maraviroc could explain the decreased expression of immune and inflammation-related genes.

Switching to raltegravir/maraviroc was associated with surrogate markers of systemic insulin resistance, probably ART-related. Indeed, BMI remained unmodified and increased hip circumference is generally associated with a favorable metabolic profile. Accordingly, the expression of genes involved in insulin resistance was enhanced in agreement with *in vitro* studies using raltegravir[2]. Since maraviroc has not been reported to affect insulin sensitivity in PLWH and in endothelial cells[20], it is reasonable to hypothesize that the gene profile favoring insulin resistance is related to raltegravir. Clinical studies report discrepant data. We recently reported increased insulin resistance in patients switching from a PI-based regimen to raltegravir-etravirine[21] while, in a similar context, authors concluded that raltegravir increased insulin sensitivity[4].

AT fibrosis adversely impacts metabolic parameters[22]. We did not observe any modification in the level of global fibrosis in SCAT and only a few genes which expression was modified were directly related to collagen remodeling. We previously reported increased fibrosis in SCAT of INSTI-treated severely obese PLWH[2]. However, maraviroc reduces fibrosis in the liver, and is now evaluated in that setting in clinical trials in PLWH with non-alcoholic-fatty-liver disease[10, 11]. It might also be anti-fibrotic on AT. Possibly, treatment with both raltegravir and maraviroc could be globally neutral regarding AT fibrosis.

Circulating levels of adipokines and cytokines remained unchanged but our study lacked potency. Clinical trials using raltegravir or dolutegravir report, or not, modification in the level of these markers[4, 5, 23]. Likewise, maraviroc markedly improved atherosclerotic progression in HIV-suppressed PLWH at high cardiovascular risk[8], but the beneficial effect on the arterial wall was local and not associated with decreased inflammatory systemic markers.

Our study has limitations. Due to premature discontinuation, a small number of patients was enrolled. However, patients monitoring was careful with reliable AT samples withdrawn before and 6 months after the switch, allowing individual comparison. We could not verify the individual level of gene expression nor the change in protein expression and therefore our propositions regarding gene expression variations remain hypothetical. We cannot address the effect of raltegravir *versus* maraviroc. As well, we cannot analyze the effect of each ART molecules received before switching. Insulin resistance was evaluated by using the surrogate QUICKI index based only on fasting glucose and insulin levels but which was shown more accurate than HOMA-IR[15].

In conclusion, in a small group of well-controlled PLWH, we observed that raltegravir/maraviroc markedly altered AT transcriptome suggesting increased adipogenesis, probably latter resulting in fat mass gain. Also, insulin resistance increased stressing for the risk of diabetes, requiring a careful follow-up. However, we observed a striking reduction in the expression of immune/inflammation-related genes. These

preliminary lead to interesting hypotheses which need to be confirmed in larger studies as they may impact the use of INSTI in some populations.

Legend of figures

Figure 1: Network analysis with the GO biological process annotation of genes with altered expression 6 months after switch to raltegravir/maraviroc

Green: decreased expression

Red: increased expression

Supplemental Figure 1: Significance Analysis of Microarrays (SAM) analysis of comparative adipose tissue gene expression after versus before the switch to raltegravir/maraviroc

Supplemental Figure 2: Functional analysis by using the KEGG database of adipose tissue genes up- or down-regulated after switch to raltegravir/maraviroc

Green: decreased expression

Red: increased expression

Acknowledgements

We thank the clinical research department from ANRS for their support regarding the management of the ROCnRAL study. We thank Ginette Marlin for evaluation of the adipokines and inflammatory markers.

JPB performed all the lipoaspirations.

VP, RA, JPB, SF, EC and EP have performed all the assays presented in this paper and participated to their analysis.

LA has monitored the ROCnRAL study

VP, LA, JPB and JC have performed the analysis of the data

CK has participated to the study as the PI of the ROCnRAL study

JPB, JC, CK and KC have written the grant proposition

JC has written the first draft, BF, JAW, KC and CK have participated to the redaction and all the authors have participated to the correction of the paper

References

1. Koethe JR, Lagathu C, Lake JE, Domingo P, Calmy A, Falutz J, et al. **HIV and antiretroviral therapy-related fat alterations**. *Nat Rev Dis Primers* 2020; 6(1):48.

2. Gorwood J, Bourgeois C, Pourcher V, Pourcher G, Charlotte F, Mantecon M, et al. **The integrase inhibitors dolutegravir and raltegravir exert pro-adipogenic and profibrotic effects and induce insulin resistance in human/simian adipose tissue and human adipocytes**. *Clin Infect Dis* 2020.

3. Katlama C, Assoumou L, Valantin MA, Soulie C, Duvivier C, Chablais L, et al. **Maraviroc plus raltegravir failed to maintain virological suppression in HIV-infected patients with lipohypertrophy: results from the ROCnRAL ANRS 157 study**. *J Antimicrob Chemother* 2014; 69(6):1648-1652.

4. Martinez E, D'Albuquerque PM, Llibre JM, Gutierrez F, Podzamczer D, Antela A, et al. **Changes in cardiovascular biomarkers in HIV-infected patients switching from ritonavir-boosted protease inhibitors to raltegravir**. *AIDS* 2012; 26(18):2315-2326.

5. Katlama C, Assoumou L, Valantin MA, Soulie C, Martinez E, Beniguel L, et al. **Dual therapy combining raltegravir with etravirine maintains a high level of viral suppression over 96 weeks in long-term experienced HIV-infected individuals over 45 years on a PI-based regimen: results from the Phase II ANRS 163 ETRAL study**. *J Antimicrob Chemother* 2019; 74(9):2742-2751.

6. Gatell JM, Assoumou L, Moyle G, Waters L, Johnson M, Domingo P, et al. **Immediate Versus Deferred Switching From a Boosted Protease Inhibitor-based Regimen to a Dolutegravir-based Regimen in Virologically Suppressed Patients With High**

Cardiovascular Risk or Age >/=50 Years: Final 96-Week Results of the NEAT022 Study. *Clin Infect Dis* 2019; 68(4):597-606.

7. Assoumou L, di Clemente N, Fellahi S, Beniguel L, Bastard JP, Feve B, et al. **Impact of the reproductive/hormonal status on weight, fat and insulin resistance in HIV-infected women switching from a PI regimen to dual raltegravir-etravirine therapy: results from the ANRS163-ETRAL trial at 48 and 96 weeks**. *HIV Med* 2019; 20(SI 9):132.

8. Francisci D, Pirro M, Schiaroli E, Mannarino MR, Cipriani S, Bianconi V, et al. **Maraviroc Intensification Modulates Atherosclerotic Progression in HIV-Suppressed Patients at High Cardiovascular Risk. A Randomized, Crossover Pilot Study**. *Open Forum Infect Dis* 2019; 6(4):ofz112.

9. Piconi S, Pocaterra D, Rainone V, Cossu M, Masetti M, Rizzardini G, et al. **Maraviroc Reduces Arterial Stiffness in PI-Treated HIV-infected Patients**. *Sci Rep* 2016; 6:28853.

10. Gonzalez EO, Boix V, Deltoro MG, Aldeguer JL, Portilla J, Montero M, et al. **The effects of Maraviroc on liver fibrosis in HIV/HCV co-infected patients**. *J Int AIDS Soc* 2014; 17(4 Suppl 3):19643.

11. Bradshaw D, Gilleece Y, Verma S, Abramowicz I, Bremner S, Perry N. **Protocol for a phase IV, open-label feasibility study investigating non-invasive markers of hepatic fibrosis in people living with HIV-1 and non-alcoholic fatty liver disease randomised to receiving optimised background therapy (OBT) plus maraviroc or OBT alone**. *BMJ Open* 2020; 10(7):e035596.

12. Bastard JP, Fellahi S, Couffignal C, Raffi F, Gras G, Hardel L, et al. **Increased systemic immune activation and inflammatory profile of long-term HIV-infected ART-controlled**

patients is related to personal factors, but not to markers of HIV infection severity. *J Antimicrob Chemother* 2015; 70(6):1816-1824.

13. Gorwood J, Bourgeois C, Mantecon M, Atlan M, Pourcher V, Pourcher G, et al. **Impact of HIV/simian immunodeficiency virus infection and viral proteins on adipose tissue fibrosis and adipogenesis**. *AIDS* 2019; 33(6):953-964.

14. Lacroix D, Moutel S, Coupaye M, Huvenne H, Faucher P, Pelloux V, et al. **Metabolic and adipose tissue signatures in adults with Prader-Willi syndrome: a model of extreme adiposity**. *J Clin Endocrinol Metab* 2015; 100(3):850-859.

15. Rabasa-Lhoret R, Bastard JP, Jan V, Ducluzeau P, Andreelli F, Guerbre F, et al. **Modified quantitative insulin sensitivity check index is better correlated to hyperinsulinemic glucose clamp than other fasting-based index of insulin sesnitivity in different insulin-resistant states**. *J Clin Endocrinol Metab* 2003; 88(10):4917-4923.

16. Diaz-Delfin J, Domingo P, Giralt M, Villarroya F. **Maraviroc reduces cytokine expression and secretion in human adipose cells without altering adipogenic differentiation**. *Cytokine* 2013; 61(3):808-815.

17. Pourcher V, Dutoit Y, Capeau J, Boccara F, Soulie C, Ndoadoumgue A, et al. **Characteristics of HIV+ and HIV- patients undergoing bariatric surgery: ObeVIH study**. In: *virtual CROI scientific spotlight-TM ID1717*. virtual; 2021.

18. Guaraldi G, Draisci J, Milic J, Carli F, Besutti G, Bassoli C, et al. **Fat distribution and ensity in people living with HIV with ≥5% weight gain**. *J Intern AIDS Soc* 2020; 23(S7):E25616.

19. Perez-Matute P, Pichel JG, Iniguez M, Recio-Fernandez E, Perez-Martinez L, Torrens R, et al. **Maraviroc ameliorates the increased adipose tissue macrophage recruitment**

induced by a high-fat diet in a mouse model of obesity. *Antivir Ther* 2017; 22(2):163-168.

20. Auclair M, Guenantin AC, Fellahi S, Garcia M, Capeau J. **HIV antiretroviral drugs, dolutegravir, maraviroc and ritonavir-boosted atazanavir use different pathways to affect inflammation, senescence and insulin sensitivity in human coronary endothelial cells**. *PLoS One* 2020; 15(1):e0226924.

21. Assoumou L, Racine C, Fellahi S, Lamaziere A, Farabos D, Beniguel L, et al. **Fat gain differs by sex and hormonal status in persons living with suppressed HIV switched to raltegravir/etravirine**. *AIDS* 2020; 34(12):1859-1862.

22. Divoux A, Tordjman J, Lacasa D, Veyrie N, Hugol D, Aissat A, et al. **Fibrosis in human adipose tissue: composition, distribution, and link with lipid metabolism and fat mass loss**. *Diabetes* 2010; 59(11):2817-2825.

23. Martinez E, Assoumou L, Moyle G, Waters L, Johnson M, Domingo P, et al. **48-week changes in biomarkers in subjects with high cardiovascular risk boosted switching from ritonavir-protease inhibitors to dolutegravir: the NEAT022 study**. *Journal of the International AIDS Society* 2018; 21(S8):e25187.

Table 1

Characteristics of PLWH included in the ROCnRAL sub-study with paired adipose tissue biopsies: clinical and metabolic parameters, adipokines and inflammatory markers, adipose tissue parameters.

The results are expressed as mean (SEM). The differences between T0 (inclusion) and T*end* was calculated by using the Wilcoxon-paired test.

	T0	T*end*	*P*
CD4 cells/mm^3	699 (56)	612 (23)	0.219
CD8 cells/mm^3	786 (100)	820 (111)	0.359
BMI kg/m^2	26.1 (1.2)	26.4 (1.3)	0.578
WC cm	94.6 (2.2)	97.9 (4.0)	0.250
HC cm	94.9 (1.8)	99.1 (2.1)	**0.031**
WHR	1.00 (0.02)	0.98 (0.02)	0.250
Trunk fat kg	13.2 (1.4)	13.6 (1.8)	0.562
Limb fat kg	8.0 (1.2)	8.1 (1.2)	0.312
Glycemia mmol/L	5.1 (0.2)	5.5 (0.25)	0.250
Triglycerides mmol/L	2.0 (0.9)	1.3 (0.2)	0.437
HDL-cholesterol mmol/L	1.35 (0.14)	1.5 (0.12)	0.219
LDL-cholesterol mmol/L	3.3 (0.33)	2.8 (0.24)	0.219
Insulinemia mU/L	10.7 (1.8)	21.5 (10.0)	**0.047**
QUICKI	0.342 (0.011)	0.315 (0.017)	**0.046**

hsCRP mg/L	2.61 (1.06)	3.8 (1.7)	0.578
hsIL-6 pg/L	4.5 (2.5)	2.7 (0.9)	0.937
Adiponectin mg/L	3.9 (0.8)	4.4 (1.1)	0.937
Leptin μg/L	12.4 (4.4)	18.2 (5.1)	0.078
sCD14 ng/ml	1583 (71)	1471 (101)	0.219
sCD163 ng/ml	699 (103)	790 (151)	0.467
Adipocyte diameter μm	106.9 (2.1)	113 (4.1)	0.109
Adipocyte volume $x10^3 \mu m^3$	649 (38)	776 (78)	0.109
Adipose tissue fibrosis AU	1.37 (0.26)	1.56 (0.35)	0.999

WC: waist circumference, HC: hip circumference, WHR: waist to hip ratio, HDL: high density lipoproteins, LDL: low density lipoproteins, AU: arbitrary unit

Figure 1

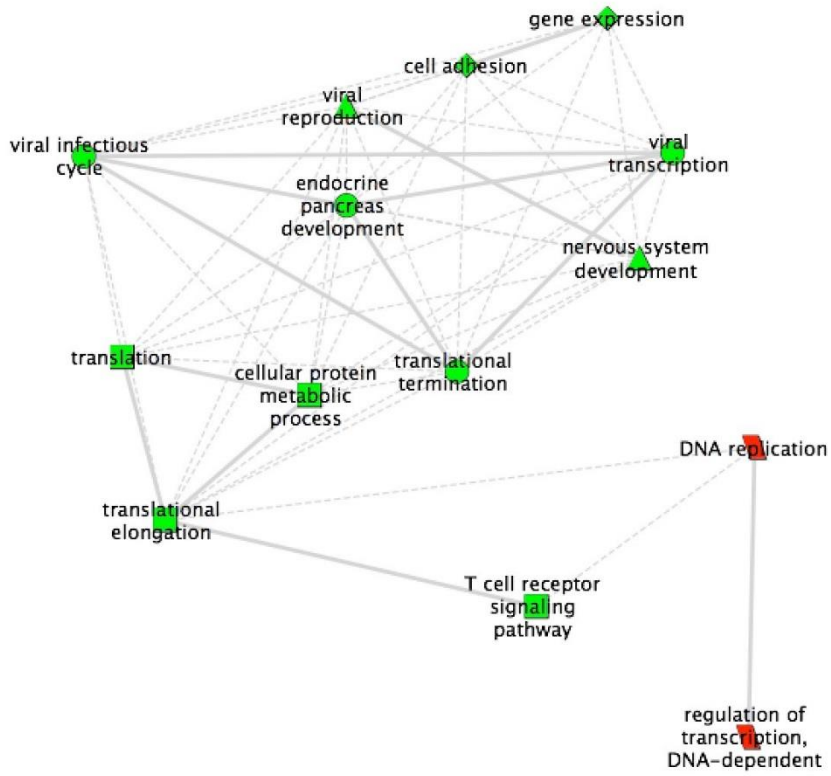

Green: decreased expression
Red: increased expression

Gene ID	ID	Gene symbol	Name	Fold Change	p-value(%
ILMN_16829	4818	NKG7	natural killer cell group 7 sequence	0,7	1,8141
ILMN_23776	919	CD247	CD247 molecule	0,7	1,2499
ILMN_21206	7102	TSPAN7	tetraspanin 7	0,7	1,8141
ILMN_16768	84417	C2orf40	chromosome 2 open reading frame 40	0,7	2,0799
ILMN_21094	3002	GZMB	granzyme B (granzyme 2, cytotoxic T-ly	0,7	2,0799
ILMN_17695	83700	JAM3	junctional adhesion molecule 3	0,7	1,5007
ILMN_17494	8502	PKP4	plakophilin 4	0,7	2,0799
ILMN_21122	7293	TNFRSF4	tumor necrosis factor receptor superfa	0,7	2,6244
ILMN_22090	6231	RPS26	ribosomal protein S26	0,7	2,0799
ILMN_16769	919	CD247	CD247 molecule	0,7	1,5007
ILMN_20862	114826	SMYD4	SET and MYND domain containing 4	0,7	2,0799
ILMN_17875	8848	TSC22D1	TSC22 domain family, member 1	0,7	1,2499
ILMN_32368	57523	NYNRIN	NYN domain and retroviral integrase cc	0,7	2,0799
ILMN_24063	10616	RBCK1	RanBP-type and C3HC4-type zinc finger	0,7	2,0799
ILMN_17707	83543	AIF1L	allograft inflammatory factor 1-like	0,7	2,0799
ILMN_32517	79002	C19orf43	chromosome 19 open reading frame 43	0,7	2,6244
ILMN_22614	915	CD3D	CD3d molecule, delta (CD3-TCR comple	0,7	1,2499
ILMN_21123	10589	DRAP1	DR1-associated protein 1 (negative cofa	0,7	2,6244
ILMN_16723	58494	JAM2	junctional adhesion molecule 2	0,7	0,0000
ILMN_17696	5878	RAB5C	RAB5C, member RAS oncogene family	0,7	2,6244
ILMN_16913	3575	IL7R	interleukin 7 receptor	0,7	1,8141
ILMN_23162	84525	HOPX	HOP homeobox	0,7	1,5007
ILMN_17484	55303	GIMAP4	GTPase, IMAP family member 4	0,7	2,0799
ILMN_17171	3476	IGBP1	immunoglobulin (CD79A) binding prote	0,8	2,0799
ILMN_32502	29767	TMOD2	tropomodulin 2 (neuronal)	0,8	1,8141
ILMN_17816	716	C1S	complement component 1, s subcompc	0,8	1,8141
ILMN_17761	283298	OLFML1	olfactomedin-like 1	0,8	0,8244
ILMN_31889	441951	C20orf199	ZNFX1 antisense RNA 1 (non-protein co	0,8	1,0331
ILMN_32433	343990	C2orf55	chromosome 2 open reading frame 55	0,8	0,0000
ILMN_17319	6329	SCN4A	sodium channel, voltage-gated, type IV	0,8	1,8141
ILMN_16704	79171	RBM42	RNA binding motif protein 42	0,8	2,6244
ILMN_21748	146894	CD300LG	CD300 molecule-like family member g	0,8	2,0799
ILMN_17852	965	CD58	CD58 molecule	0,8	2,0799
ILMN_18057	5214	PFKP	phosphofructokinase, platelet	0,8	2,6244
ILMN_16875	10507	SEMA4D	sema domain, immunoglobulin domain	0,8	1,2499
ILMN_16512	255877	BCL6B	B-cell CLL/lymphoma 6, member B	0,8	2,6244
ILMN_16984	3609	ILF3	interleukin enhancer binding factor 3, 9	0,8	2,0799
ILMN_23882	9862	MED24	mediator complex subunit 24	0,8	2,6244
ILMN_18060	5720	PSME1	proteasome (prosome, macropain) acti	0,8	2,6244
ILMN_23841	9289	GPR56	G protein-coupled receptor 56	0,8	1,8141
ILMN_17695	54453	RIN2	Ras and Rab interactor 2	0,8	2,0799
ILMN_17545	9828	ARHGEF17	Rho guanine nucleotide exchange facto	0,8	1,5007
ILMN_16890	79673	ZNF329	zinc finger protein 329	0,8	2,6244
ILMN_16582	6139	RPL17	ribosomal protein L17	0,8	1,8141
ILMN_32514	9804	TOMM20	translocase of outer mitochondrial mer	0,8	1,5007

ILMN_21574	3122	HLA-DRA	major histocompatibility complex, class	0,8	2,6244
ILMN_17478	6605	SMARCE1	SWI/SNF related, matrix associated, act	0,8	2,0799
ILMN_17959	116988	CENTG3	ArfGAP with GTPase domain, ankyrin re	0,8	2,6244
ILMN_23258	915	CD3D	CD3d molecule, delta (CD3-TCR comple	0,8	2,6244
ILMN_16857	1974	EIF4A2	eukaryotic translation initiation factor 4	0,8	1,5007
ILMN_18044	57228	SMAGP	small cell adhesion glycoprotein	0,8	1,5007
ILMN_18134	5092	PCBD1	pterin-4 alpha-carbinolamine dehydrat	0,8	2,6244
ILMN_16535	1901	EDG1	sphingosine-1-phosphate receptor 1	0,8	2,6244
ILMN_17217	54707	ATPBD1B	GPN-loop GTPase 2	0,8	2,6244
ILMN_32438	4695	NDUFA2	NADH dehydrogenase (ubiquinone) 1 a	0,8	1,0331
ILMN_16608	6050	RNH1	ribonuclease/angiogenin inhibitor 1	0,8	2,6244
ILMN_17303	84317	CCDC115	coiled-coil domain containing 115	0,8	2,0799
ILMN_16597	689	BTF3	basic transcription factor 3	0,8	1,5007
ILMN_22537	7903	ST8SIA4	ST8 alpha-N-acetyl-neuraminide alpha-	0,8	1,8141
ILMN_21202	10231	RCAN2	regulator of calcineurin 2	0,8	2,6244
ILMN_17433	113189	CHST14	carbohydrate (N-acetylgalactosamine 4	0,8	2,6244
ILMN_17592	118	ADD1	adducin 1 (alpha)	0,8	1,2499
ILMN_16768	116835	HSPA12B	heat shock 70kD protein 12B	0,8	1,8141
ILMN_17690	5547	PRCP	prolylcarboxypeptidase (angiotensinase	0,8	2,0799
ILMN_23402	5142	PDE4B	phosphodiesterase 4B, cAMP-specific	0,8	0,0000
ILMN_18007	23180	RFTN1	raftlin, lipid raft linker 1	0,8	2,6244
ILMN_23372	6210	RPS15A	ribosomal protein S15a	0,8	1,0331
ILMN_16780	9425	CDYL	chromodomain protein, Y-like	0,8	1,8141
ILMN_16590	3111	HLA-DOA	major histocompatibility complex, class	0,8	1,8141
ILMN_18083	9744	ACAP1	ArfGAP with coiled-coil, ankyrin repeat	0,8	2,0799
ILMN_16804	6748	SSR4	signal sequence receptor, delta	0,8	2,6244
ILMN_20796	3820	KLRB1	killer cell lectin-like receptor subfamily	0,8	1,2499
ILMN_18129	116159	CYYR1	cysteine/tyrosine-rich 1	0,8	2,0799
ILMN_17973	23048	FNBP1	formin binding protein 1	0,8	2,0799
ILMN_17823	5430	POLR2A	polymerase (RNA) II (DNA directed) pol	0,8	1,5007
ILMN_22050	57692	MAGEE1	melanoma antigen family E, 1	0,8	2,0799
ILMN_23520	9289	GPR56	G protein-coupled receptor 56	0,8	0,0000
ILMN_17917	1375	CPT1B	carnitine palmitoyltransferase 1B (musc	0,8	2,6244
ILMN_16797	104	ADARB1	adenosine deaminase, RNA-specific, B1	0,8	2,6244
ILMN_23830	6139	RPL17	ribosomal protein L17	0,8	2,0799
ILMN_23251	408	ARRB1	arrestin, beta 1	0,8	0,8244
ILMN_18038	84518	CNFN	cornifelin	0,8	2,6244
ILMN_16680	90952	ESAM	endothelial cell adhesion molecule	0,8	2,6244
ILMN_17775	3695	ITGB7	integrin, beta 7	0,8	1,5007
ILMN_16657	1434	CSE1L	CSE1 chromosome segregation 1-like (y	0,8	2,6244
ILMN_23523	9770	RASSF2	Ras association (RalGDS/AF-6) domain f	0,8	2,6244
ILMN_18151	4628	MYH10	myosin, heavy chain 10, non-muscle	0,8	2,6244
ILMN_16772	55217	TMLHE	trimethyllysine hydroxylase, epsilon	0,8	2,0799
ILMN_16519	8460	TPST1	tyrosylprotein sulfotransferase 1	0,8	1,2499
ILMN_16779	51292	GMPR2	guanosine monophosphate reductase 2	0,8	1,2499
ILMN_21179	7570	ZNF22	zinc finger protein 22 (KOX 15)	0,8	2,6244

ILMN_17006(	84282	RNF135	ring finger protein 135	0,8	2,6244
ILMN_17808(	5583	PRKCH	protein kinase C, eta	0,8	0,7857
ILMN_17754(	5217	PFN2	profilin 2	0,8	2,6244
ILMN_17754(	8082	SSPN	sarcospan	0,8	2,0799
ILMN_32394(	100128927	ZBTB42	zinc finger and BTB domain containing (	0,8	1,5007
ILMN_17975(	84269	CHCHD5	coiled-coil-helix-coiled-coil-helix domai	0,8	2,6244
ILMN_21916(	51142	CHCHD2	coiled-coil-helix-coiled-coil-helix domai	0,8	2,0799
ILMN_16940(	27335	EIF3K	eukaryotic translation initiation factor 3	0,8	0,8244
ILMN_17813(	5239	PGM5	phosphoglucomutase 5	0,8	1,8141
ILMN_17513(	10616	RBCK1	RanBP-type and C3HC4-type zinc finger	0,8	1,8141
ILMN_16557(	54460	MRPS21	mitochondrial ribosomal protein S21	0,8	1,8141
ILMN_17831(	6192	RPS4Y1	ribosomal protein S4, Y-linked 1	0,8	1,5007
ILMN_23265(	834	CASP1	caspase 1, apoptosis-related cysteine p	0,8	2,6244
ILMN_20870(	54543	TOMM7	translocase of outer mitochondrial mer	0,8	2,0799
ILMN_17395(	78987	CRELD1	cysteine-rich with EGF-like domains 1	0,8	1,2499
ILMN_17095(	5239	PGM5	phosphoglucomutase 5	0,8	1,8141
ILMN_18113(	2494	NR5A2	nuclear receptor subfamily 5, group A,	0,8	1,8141
ILMN_17761(	5414	38231	septin 4	0,8	1,8141
ILMN_17357(	3764	KCNJ8	potassium inwardly-rectifying channel,	0,8	2,0799
ILMN_17558(	85360	SYDE1	synapse defective 1, Rho GTPase, homo	0,8	2,0799
ILMN_20876(	79901	CYBRD1	cytochrome b reductase 1	0,8	2,0799
ILMN_23826(	11043	MID2	midline 2	0,8	2,0799
ILMN_21676(	4666	NACA	nascent polypeptide-associated comple	0,8	2,0799
ILMN_21545(	4736	RPL10A	ribosomal protein L10a	0,8	2,0799
ILMN_16711(	2701	GJA4	gap junction protein, alpha 4, 37kDa	0,8	1,0331
ILMN_23345(	3183	HNRNPC	heterogeneous nuclear ribonucleoprot	0,8	2,0799
ILMN_16568(	5947	RBP1	retinol binding protein 1, cellular	0,8	2,6244
ILMN_16990(	8550	MAPKAPK5	mitogen-activated protein kinase-activa	0,8	1,0331
ILMN_21399(	6189	RPS3A	ribosomal protein S3A	0,8	0,8244
ILMN_17365(	151473	SLC16A14	solute carrier family 16, member 14 (m	0,8	1,5007
ILMN_17116(	25824	PRDX5	peroxiredoxin 5	0,8	1,5007
ILMN_22269(	9766	KIAA0247	KIAA0247	0,8	2,0799
ILMN_23685(	115290	FBXO17	F-box protein 17	0,8	2,0799
ILMN_17115(	1690	COCH	coagulation factor C homolog, cochlin (	0,8	1,2499
ILMN_17612(	2132	EXT2	exostosin 2	0,8	1,5007
ILMN_20730(	94107	TMEM203	transmembrane protein 203	0,8	2,0799
ILMN_17496(	8454	CUL1	cullin 1	0,8	1,0331
ILMN_17164(	65057	ACD	adrenocortical dysplasia homolog (mou	0,8	1,2499
ILMN_16740(	54543	TOMM7	translocase of outer mitochondrial mer	0,8	1,2499
ILMN_23194(	689	BTF3	basic transcription factor 3	0,8	2,0799
ILMN_17627(	6138	RPL15	ribosomal protein L15	0,8	1,5007
ILMN_17651(	3455	IFNAR2	interferon (alpha, beta and omega) rec	0,8	2,6244
ILMN_17394(	5396	PRRX1	paired related homeobox 1	0,8	2,6244
ILMN_16920(	4692	NDN	necdin homolog (mouse)	0,8	2,6244
ILMN_17494(	64983	MRPL32	mitochondrial ribosomal protein L32	0,8	1,8141
ILMN_18104(	83871	RAB34	RAB34, member RAS oncogene family	0,8	1,2499

ILMN_17306	408	ARRB1	arrestin, beta 1	0,8	2,0799
ILMN_18102	90423	ATP6V1E2	ATPase, H+ transporting, lysosomal 31k	0,8	2,0799
ILMN_21012	64407	RGS18	regulator of G-protein signaling 18	0,8	1,5007
ILMN_32453	84747	UNC119B	unc-119 homolog B (C. elegans)	0,8	2,6244
ILMN_18116	117246	FTSJ3	FtsJ homolog 3 (E. coli)	0,8	2,6244
ILMN_16801	55353	LAPTM4B	lysosomal protein transmembrane 4 be	0,8	2,0799
ILMN_17611	286257	C9orf142	chromosome 9 open reading frame 142	0,8	1,2499
ILMN_17145	79026	AHNAK	AHNAK nucleoprotein	0,8	0,0000
ILMN_16787	6993	DYNLT1	dynein, light chain, Tctex-type 1	0,8	2,0799
ILMN_24002	6717	SRI	sorcin	0,8	2,6244
ILMN_17601	11043	MID2	midline 2	0,8	1,8141
ILMN_17204	5253	PHF2	PHD finger protein 2	0,8	1,8141
ILMN_18031	23450	SF3B3	splicing factor 3b, subunit 3, 130kDa	0,8	1,2499
ILMN_18026	83468	GLT8D2	glycosyltransferase 8 domain containin	0,8	1,8141
ILMN_20873	55113	XKR8	XK, Kell blood group complex subunit-r	0,8	1,5007
ILMN_32388	23248	RPRD2	regulation of nuclear pre-mRNA domai	0,8	0,0000
ILMN_18089	6194	RPS6	ribosomal protein S6	0,8	1,2499
ILMN_17383	1938	EEF2	eukaryotic translation elongation factor	0,8	2,0799
ILMN_18007	6167	RPL37	ribosomal protein L37	0,8	2,6244
ILMN_23159	81606	LBH	limb bud and heart development homo	0,8	2,0799
ILMN_16523	222223	KIAA1324L	KIAA1324-like	0,8	2,6244
ILMN_17247	8440	NCK2	NCK adaptor protein 2	0,9	1,5007
ILMN_16593	26610	ELP4	elongation protein 4 homolog (S. cerev	0,9	2,6244
ILMN_17375	6874	TAF4	TAF4 RNA polymerase II, TATA box binc	0,9	1,8141
ILMN_17845	6383	SDC2	syndecan 2	0,9	2,6244
ILMN_17202	64806	IL25	interleukin 25	0,9	0,8244
ILMN_17189	9802	DAZAP2	DAZ associated protein 2	0,9	0,0000
ILMN_17490	3115	HLA-DPB1	major histocompatibility complex, class	0,9	2,0799
ILMN_17629	9812	KIAA0141	KIAA0141	0,9	1,2499
ILMN_17719	57153	SLC44A2	solute carrier family 44, member 2	0,9	1,8141
ILMN_17671	54816	ZNF280D	zinc finger protein 280D	0,9	1,8141
ILMN_17421	83743	GRWD1	glutamate-rich WD repeat containing 1	0,9	1,0331
ILMN_16525	89853	FAM125B	family with sequence similarity 125, me	0,9	1,2499
ILMN_17287	221395	GPR116	G protein-coupled receptor 116	0,9	2,6244
ILMN_17734	6764	ST5	suppression of tumorigenicity 5	0,9	2,0799
ILMN_16900	9270	ITGB1BP1	integrin beta 1 binding protein 1	0,9	2,6244
ILMN_17737	65005	MRPL9	mitochondrial ribosomal protein L9	0,9	2,6244
ILMN_21018	55353	LAPTM4B	lysosomal protein transmembrane 4 be	0,9	1,8141
ILMN_17313	55486	PARL	presenilin associated, rhomboid-like	0,9	1,5007
ILMN_32395	401115	C4orf48	chromosome 4 open reading frame 48	0,9	2,6244
ILMN_17022	79630	C1orf54	chromosome 1 open reading frame 54	0,9	2,6244
ILMN_17791	23384	CYTSA	sperm antigen with calponin homology	0,9	2,0799
ILMN_17291	55069	C7orf42	transmembrane protein 248	0,9	2,6244
ILMN_16827	8463	TEAD2	TEA domain family member 2	0,9	1,0331
ILMN_17975	116841	SNAP47	synaptosomal-associated protein, 47kD	0,9	2,0799
ILMN_16893	83443	SF3B5	splicing factor 3b, subunit 5, 10kDa	0,9	2,0799

ILMN_17397	126792	B3GALT6	UDP-Gal:betaGal beta 1,3-galactosyltra	0,9	2,6244
ILMN_17063	51241	C14orf112	COX16 cytochrome c oxidase assembly	0,9	2,6244
ILMN_17618	90411	MCFD2	multiple coagulation factor deficiency 2	0,9	2,0799
ILMN_17172	10544	PROCR	protein C receptor, endothelial	0,9	2,0799
ILMN_16830	5504	PPP1R2	protein phosphatase 1, regulatory (inhi	0,9	2,6244
ILMN_16663	93058	COQ10A	coenzyme Q10 homolog A (S. cerevisiae	0,9	2,6244
ILMN_16796	27352	SGSM3	small G protein signaling modulator 3	0,9	1,8141
ILMN_17256	6612	SUMO3	SMT3 suppressor of mif two 3 homolog	0,9	1,5007
ILMN_23521	2064	ERBB2	v-erb-b2 erythroblastic leukemia viral o	0,9	1,5007
ILMN_16743	10971	YWHAQ	tyrosine 3-monooxygenase/tryptophan	0,9	1,5007
ILMN_21988	2230	FDX1	ferredoxin 1	0,9	2,0799
ILMN_16911	116092	DNTTIP1	deoxynucleotidyltransferase, terminal,	0,9	0,8244
ILMN_24081	24144	TFIP11	tuftelin interacting protein 11	0,9	2,0799
ILMN_16765	5654	HTRA1	HtrA serine peptidase 1	0,9	0,8244
ILMN_16767	4236	MFAP1	microfibrillar-associated protein 1	0,9	2,0799
ILMN_16949	5780	PTPN9	protein tyrosine phosphatase, non-rece	0,9	2,6244
ILMN_18019	10465	PPIH	peptidylprolyl isomerase H (cyclophilin	0,9	0,8244
ILMN_16784	1123	CHN1	chimerin (chimaerin) 1	0,9	2,6244
ILMN_18129	10695	CNPY3	canopy 3 homolog (zebrafish)	0,9	2,0799
ILMN_17970	10436	EMG1	EMG1 nucleolar protein homolog (S. ce	0,9	2,0799
ILMN_22343	80772	GLTPD1	glycolipid transfer protein domain cont	0,9	1,0331
ILMN_20555	55790	CSGALNACT1	chondroitin sulfate N-acetylgalactosam	0,9	1,2499
ILMN_16702	26020	LRP10	low density lipoprotein receptor-relate	0,9	0,8244
ILMN_16971	51759	C9orf78	chromosome 9 open reading frame 78	0,9	1,5007
ILMN_17032	112970	KTI12	KTI12 homolog, chromatin associated (	0,9	2,6244
ILMN_16772	11178	LZTS1	leucine zipper, putative tumor suppress	0,9	1,8141
ILMN_16934	23478	SEC11A	SEC11 homolog A (S. cerevisiae)	0,9	2,6244
ILMN_18075	55181	C17orf71	smg-8 homolog, nonsense mediated m	0,9	1,8141
ILMN_17351	57019	CIAPIN1	cytokine induced apoptosis inhibitor 1	0,9	1,8141
ILMN_17200	30844	EHD4	EH-domain containing 4	0,9	1,2499
ILMN_17021	2739	GLO1	glyoxalase I	0,9	2,6244
ILMN_16724	6135	RPL11	ribosomal protein L11	0,9	2,6244
ILMN_16878	22928	SEPHS2	selenophosphate synthetase 2	0,9	2,6244
ILMN_16515	8603	FAM193A	family with sequence similarity 193, me	0,9	2,0799
ILMN_16692	7564	ZNF16	zinc finger protein 16	0,9	1,8141
ILMN_17433	7265	TTC1	tetratricopeptide repeat domain 1	0,9	1,0331
ILMN_16727	90550	CCDC109A	mitochondrial calcium uniporter	0,9	2,6244
ILMN_22255	27034	ACAD8	acyl-CoA dehydrogenase family, memb	0,9	1,2499
ILMN_17163	64225	ATL2	atlastin GTPase 2	0,9	1,2499
ILMN_17553	7275	TUB	tubby homolog (mouse)	0,9	0,8244
ILMN_16573	5439	POLR2J	polymerase (RNA) II (DNA directed) pol	0,9	2,0799
ILMN_21148	6135	RPL11	ribosomal protein L11	0,9	2,6244
ILMN_32483	54617	INO80	INO80 homolog (S. cerevisiae)	0,9	1,2499
ILMN_18067	140459	ASB6	ankyrin repeat and SOCS box containing	0,9	2,6244
ILMN_16542	115	ADCY9	adenylate cyclase 9	0,9	1,2499
ILMN_17308	284424	C19orf30	MIR7-3 host gene (non-protein coding)	0,9	2,0799

ILMN_17267(	55748	CNDP2	CNDP dipeptidase 2 (metallopeptidase	0,9	1,5007
ILMN_17128(	126669	SHE	Src homology 2 domain containing E	0,9	2,0799
ILMN_17751(	5136	PDE1A	phosphodiesterase 1A, calmodulin-dep	0,9	2,6244
ILMN_18123(	9168	TMSB10	thymosin beta 10	0,9	1,8141
ILMN_17047(	22918	CD93	CD93 molecule	0,9	1,5007
ILMN_16759(	3459	IFNGR1	interferon gamma receptor 1	0,9	1,8141
ILMN_16851(	54942	C9orf6	family with sequence similarity 206, me	0,9	2,0799
ILMN_17041(	207063	DHRSX	dehydrogenase/reductase (SDR family)	0,9	1,5007
ILMN_17901(	3815	KIT	v-kit Hardy-Zuckerman 4 feline sarcoma	0,9	2,6244
ILMN_16886(	10782	ZNF274	zinc finger protein 274	0,9	1,2499
ILMN_17601(	6804	STX1A	syntaxin 1A (brain)	0,9	1,8141
ILMN_16731(	79042	TSEN34	tRNA splicing endonuclease 34 homolog	0,9	2,6244
ILMN_17738(	7041	TGFB1I1	transforming growth factor beta 1 indu	0,9	2,6244
ILMN_17244(	23464	GCAT	glycine C-acetyltransferase	0,9	2,0799
ILMN_17076(	10686	CLDN16	claudin 16	0,9	1,8141

e)

Supplemental Figure 2

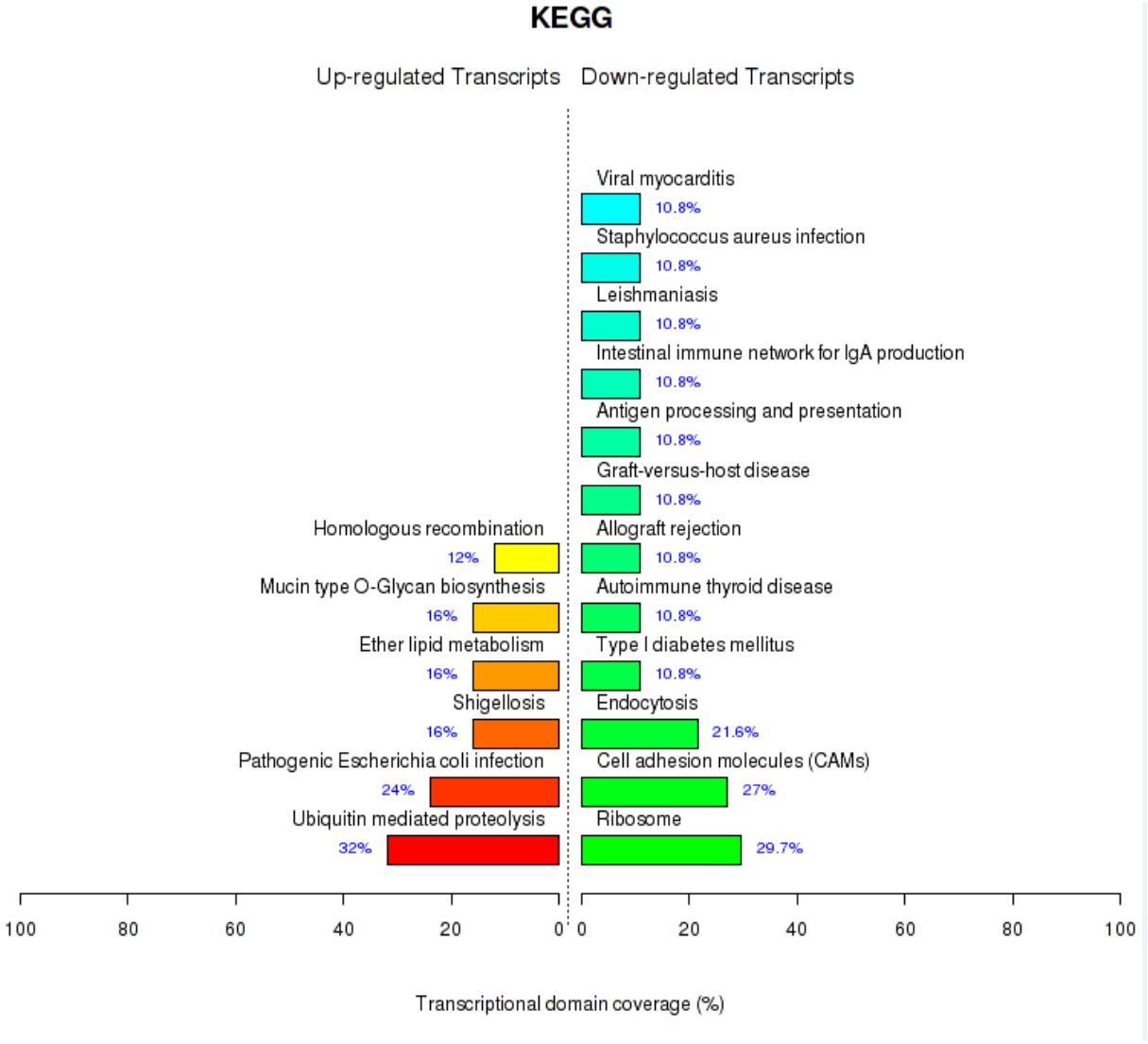

Supplemental Figure 1

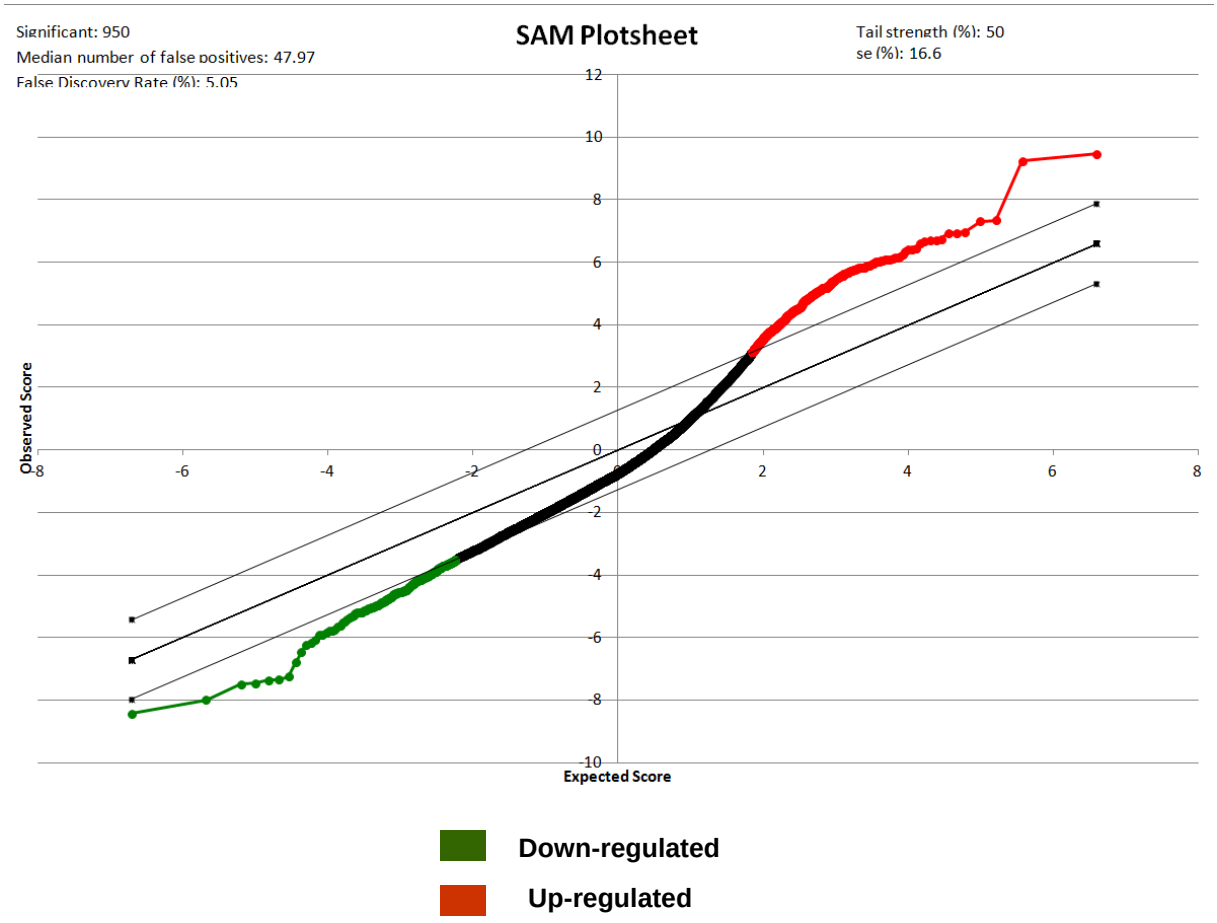

Gene ID	ID	Gene ID	NAME	Fold Chang	p-value(%
ILMN_20753	8364	HIST1H4C	histone cluster 1, H4c	10,6	1,8141
ILMN_32514	64710	NUCKS1	nuclear casein kinase and cyclin-depen	8,6	1,0331
ILMN_21135	51449	PCYOX1	prenylcysteine oxidase 1	7,7	1,5007
ILMN_21300	91368	CDKN2AIPNL	CDKN2A interacting protein N-terminal	7,7	0,3847
ILMN_16613	6711	SPTBN1	spectrin, beta, non-erythrocytic 1	6,8	1,5007
ILMN_21159	84124	ZNF394	zinc finger protein 394	6,3	1,8141
ILMN_24157	26118	WSB1	WD repeat and SOCS box containing 1	6,3	1,2499
ILMN_20519	126272	EID2B	EP300 interacting inhibitor of different	6,1	1,2499
ILMN_21137	157777	C8orf45	minichromosome maintenance domair	6,0	0,3847
ILMN_32371	84142	FAM175A	family with sequence similarity 175, me	6,0	0,6097
ILMN_22274	256051	ZNF549	zinc finger protein 549	5,9	1,5007
ILMN_16921	7561	ZNF14	zinc finger protein 14	5,8	0,3847
ILMN_23138	91120	ZNF682	zinc finger protein 682	5,7	0,7969
ILMN_21768	7620	ZNF69	zinc finger protein 69	5,7	1,8141
ILMN_21502	55033	FKBP14	FK506 binding protein 14, 22 kDa	5,7	1,5007
ILMN_22103	200728	TMEM17	transmembrane protein 17	5,6	1,8141
ILMN_21107	1138	CHRNA5	cholinergic receptor, nicotinic, alpha 5	5,6	1,5007
ILMN_17224	142679	DUSP19	dual specificity phosphatase 19	5,6	1,8141
ILMN_22860	117155	CATSPER2	cation channel, sperm associated 2	5,5	0,3847
ILMN_22153	317781	DDX51	DEAD (Asp-Glu-Ala-Asp) box polypeptic	5,5	0,3847
ILMN_17350	1316	KLF6	Kruppel-like factor 6	5,5	1,5007
ILMN_32416	84109	QRFPR	pyroglutamylated RFamide peptide rec	5,5	0,7969
ILMN_21225	147372	CCBE1	collagen and calcium binding EGF dom	5,4	0,3847
ILMN_16615	54741	LEPROT	leptin receptor overlapping transcript	5,4	0,6097
ILMN_21881	339231	ARL16	ADP-ribosylation factor-like 16	5,3	0,3847
ILMN_17213	84061	MAGT1	magnesium transporter 1	5,3	1,0331
ILMN_32381	399761	BMS1P5	BMS1 pseudogene 5	5,3	0,7969
ILMN_22061	57477	SHROOM4	shroom family member 4	5,2	1,8141
ILMN_22357	56850	GRIPAP1	GRIP1 associated protein 1	5,1	1,0331
ILMN_22049	7516	XRCC2	X-ray repair complementing defective r	5,0	1,5007
ILMN_23342	1385	CREB1	cAMP responsive element binding prot	5,0	1,2499
ILMN_22857	55775	TDP1	tyrosyl-DNA phosphodiesterase 1	5,0	1,8141
ILMN_21543	9723	SEMA3E	sema domain, immunoglobulin domair	4,9	2,0799
ILMN_22357	81033	KCNH6	potassium voltage-gated channel, subf	4,9	0,3847
ILMN_17510	162073	ITPRIPL2	inositol 1,4,5-trisphosphate receptor in	4,9	1,0331
ILMN_22301	641737	FLJ44124	uncharacterized LOC641737	4,9	0,3847
ILMN_17857	56203	LMOD3	leiomodin 3 (fetal)	4,8	1,5007
ILMN_20787	84334	C14orf153	apoptogenic 1	4,8	1,2499
ILMN_17104	5700	PSMC1	proteasome (prosome, macropain) 26S	4,8	0,7969
ILMN_20785	154791	HSPC268	chromosome 7 open reading frame 55	4,7	1,0331
ILMN_21623	11144	DMC1	DMC1 dosage suppressor of mck1 hom	4,7	1,5007
ILMN_21948	649598	FLJ46309	hypothetical protein LOC649598	4,7	0,3847
ILMN_21284	1601	DAB2	disabled homolog 2, mitogen-responsiv	4,7	1,5007
ILMN_21233	64167	LRAP	endoplasmic reticulum aminopeptidase	4,7	1,2499
ILMN_21175	64789	DEM1	defects in morphology 1 homolog (S. ce	4,7	1,2499

ILMN_20757	126205	NLRP8	NLR family, pyrin domain containing 8	4,7	0,3847
ILMN_17724	92014	MCART1	solute carrier family 25, member 51	4,6	0,3847
ILMN_17360	79693	YRDC	yrdC domain containing (E. coli)	4,5	0,7969
ILMN_16914	5718	PSMD12	proteasome (prosome, macropain) 26S	4,5	0,6097
ILMN_16797	51449	PCYOX1	prenylcysteine oxidase 1	4,4	1,5007
ILMN_20911	80867	HCG2P7	HLA complex group 2 pseudogene 7	4,3	1,2499
ILMN_21397	22998	LIMCH1	LIM and calponin homology domains 1	4,3	1,5007
ILMN_20493	151194	FAM119A	methyltransferase like 21A	4,2	1,2499
ILMN_23611	64393	ZMAT3	zinc finger, matrin-type 3	4,2	1,5007
ILMN_17374	1316	KLF6	Kruppel-like factor 6	4,2	2,0799
ILMN_16802	25862	USP49	ubiquitin specific peptidase 49	4,1	0,3847
ILMN_32354	84278	HIATL2	hippocampus abundant transcript-like	4,1	1,0331
ILMN_20735	25764	C15orf63	chromosome 15 open reading frame 63	4,1	1,2499
ILMN_21178	503632	DUXAP3	double homeobox A pseudogene 3	4,1	1,0331
ILMN_21504	64417	C5orf28	chromosome 5 open reading frame 28	4,1	1,2499
ILMN_22798	158399	ZNF483	zinc finger protein 483	4,1	1,5007
ILMN_24078	54756	IL17RD	interleukin 17 receptor D	4,0	0,7969
ILMN_21066	8548	BLZF1	basic leucine zipper nuclear factor 1	4,0	1,5007
ILMN_32456	147172	LRRC37B2	leucine rich repeat containing 37B pseu	4,0	1,0331
ILMN_16801	10087	COL4A3BP	collagen, type IV, alpha 3 (Goodpasture	4,0	1,2499
ILMN_32251	148203	ZNF738	zinc finger protein 738	4,0	1,0331
ILMN_22793	2204	FCAR	Fc fragment of IgA, receptor for	4,0	2,6244
ILMN_22494	10558	SPTLC1	serine palmitoyltransferase, long chain	4,0	0,3847
ILMN_16937	250	ALPP	alkaline phosphatase, placental	3,9	1,2499
ILMN_16817	2309	FOXO3	forkhead box O3	3,9	1,8141
ILMN_32443	202243	CCDC125	coiled-coil domain containing 125	3,9	0,6097
ILMN_24011	9698	PUM1	pumilio homolog 1 (Drosophila)	3,9	1,2499
ILMN_22767	23509	POFUT1	protein O-fucosyltransferase 1	3,9	1,8141
ILMN_23701	3192	HNRNPU	heterogeneous nuclear ribonucleoprot	3,8	1,2499
ILMN_17449	22836	RHOBTB3	Rho-related BTB domain containing 3	3,8	1,5007
ILMN_18121	8396	PIP5K2B	phosphatidylinositol-5-phosphate 4-kir	3,7	0,3847
ILMN_21066	8548	BLZF1	basic leucine zipper nuclear factor 1	3,7	0,7969
ILMN_32363	205327	C2orf69	chromosome 2 open reading frame 69	3,7	0,7969
ILMN_23815	27297	CRCP	CGRP receptor component	3,7	0,3847
ILMN_22117	400866	C21orf24	long intergenic non-protein coding RNA	3,6	1,2499
ILMN_20591	79939	SLC35E1	solute carrier family 35, member E1	3,6	0,3847
ILMN_18141	6925	TCF4	transcription factor 4	3,6	1,2499
ILMN_16716	51478	HSD17B7	hydroxysteroid (17-beta) dehydrogena	3,6	1,2499
ILMN_17985	84515	MCM8	minichromosome maintenance comple	3,6	0,3847
ILMN_16977	55333	SYNJ2BP	synaptojanin 2 binding protein	3,6	1,2499
ILMN_20545	285605	DTWD2	DTW domain containing 2	3,6	0,3847
ILMN_33078	54058	C21orf58	chromosome 21 open reading frame 58	3,5	0,6097
ILMN_16894	26137	ZBTB20	zinc finger and BTB domain containing	3,5	1,0331
ILMN_21235	374986	FAM73A	family with sequence similarity 73, mer	3,5	0,3847
ILMN_23342	1385	CREB1	cAMP responsive element binding prot	3,5	0,6097
ILMN_20549	63929	XPNPEP3	X-prolyl aminopeptidase (aminopeptid	3,4	1,5007

ILMN_23304	54940	OCIAD1	OCIA domain containing 1	3,4	0,3847
ILMN_22128	84765	ZNF577	zinc finger protein 577	3,4	1,5007
ILMN_20790	58493	C9orf80	chromosome 9 open reading frame 80	3,4	0,6097
ILMN_23424	27068	PPA2	pyrophosphatase (inorganic) 2	3,3	0,3847
ILMN_20910	157657	C8orf37	chromosome 8 open reading frame 37	3,3	0,3847
ILMN_22884	84984	C3orf34	centrosomal protein 19kDa	3,3	1,5007
ILMN_22622	10206	TRIM13	tripartite motif containing 13	3,3	1,5007
ILMN_21581	80264	ZNF430	zinc finger protein 430	3,3	0,7969
ILMN_16980	10395	DLC1	deleted in liver cancer 1	3,3	1,0331
ILMN_16719	7360	UGP2	UDP-glucose pyrophosphorylase 2	3,2	0,7969
ILMN_21553	22834	ZNF652	zinc finger protein 652	3,2	0,3847
ILMN_17267	246243	RNASEH1	ribonuclease H1	3,2	2,0799
ILMN_32517	87178	PNPT1	polyribonucleotide nucleotidyltransfer	3,2	0,7969
ILMN_16559	9701	SAPS2	protein phosphatase 6, regulatory subu	3,1	1,8141
ILMN_20733	3586	IL10	interleukin 10	3,1	0,3847
ILMN_32492	113277	TMEM106A	transmembrane protein 106A	3,1	0,3847
ILMN_18126	4641	MYO1C	myosin IC	3,1	0,3847
ILMN_21809	387700	SLC16A12	solute carrier family 16, member 12 (m	3,1	0,3847
ILMN_22435	10838	ZNF275	zinc finger protein 275	3,0	0,3847
ILMN_16615	977	CD151	CD151 molecule (Raph blood group)	3,0	0,7969
ILMN_21052	145482	PTGR2	prostaglandin reductase 2	3,0	0,3847
ILMN_21689	8562	DENR	density-regulated protein	3,0	0,6097
ILMN_17782	285966	FLJ40722	family with sequence similarity 115, me	3,0	0,3847
ILMN_17863	3842	TNPO1	transportin 1	3,0	2,6244
ILMN_20535	54933	RHBDL2	rhomboid, veinlet-like 2 (Drosophila)	2,9	0,3847
ILMN_18056	90649	ZNF486	zinc finger protein 486	2,9	0,3847
ILMN_22221	55728	N4BP2	NEDD4 binding protein 2	2,9	0,3847
ILMN_20553	8930	MBD4	methyl-CpG binding domain protein 4	2,9	1,2499
ILMN_32450	50807	ASAP1	ArfGAP with SH3 domain, ankyrin repe	2,8	1,8141
ILMN_17137	136051	ZNF786	zinc finger protein 786	2,8	0,3847
ILMN_23974	10052	GJC1	gap junction protein, gamma 1, 45kDa	2,8	0,7969
ILMN_16943	3382	ICA1	islet cell autoantigen 1, 69kDa	2,8	0,3847
ILMN_17636	89970	RSPRY1	ring finger and SPRY domain containing	2,8	1,8141
ILMN_32266	642280	MGC26356	zinc finger protein 876, pseudogene	2,8	0,7969
ILMN_16810	10555	AGPAT2	1-acylglycerol-3-phosphate O-acyltrans	2,7	1,8141
ILMN_16919	10983	CCNI	cyclin I	2,7	1,0331
ILMN_17612	5143	PDE4C	phosphodiesterase 4C, cAMP-specific	2,7	0,3847
ILMN_17212	1438	CSF2RA	colony stimulating factor 2 receptor, al	2,7	0,3847
ILMN_23633	8740	TNFSF14	tumor necrosis factor (ligand) superfan	2,7	1,0331
ILMN_23831	27072	VPS41	vacuolar protein sorting 41 homolog (S	2,7	0,3847
ILMN_21050	26258	PLDN	pallidin homolog (mouse)	2,6	0,3847
ILMN_16670	55066	PDPR	pyruvate dehydrogenase phosphatase	2,6	1,8141
ILMN_20891	94056	SYAP1	synapse associated protein 1	2,6	0,3847
ILMN_16901	401494	PTPLAD2	protein tyrosine phosphatase-like A do	2,6	0,3847
ILMN_16590	9475	ROCK2	Rho-associated, coiled-coil containing p	2,6	1,5007
ILMN_24056	330	BIRC3	baculoviral IAP repeat containing 3	2,6	1,5007

ILMN_32516(	54813	KLHL28	kelch-like 28 (Drosophila)	2,6	1,0331
ILMN_17110	653489	LOC653489	RANBP2-like and GRIP domain containi	2,5	0,7969
ILMN_18085(	30011	SH3KBP1	SH3-domain kinase binding protein 1	2,5	1,8141
ILMN_20514(	87178	PNPT1	polyribonucleotide nucleotidyltransfer	2,5	0,6097
ILMN_21750	56165	TDRD1	tudor domain containing 1	2,5	2,0799
ILMN_18142(	54943	C21orf55	DnaJ (Hsp40) homolog, subfamily C, me	2,5	0,7969
ILMN_22435	79864	C11orf63	chromosome 11 open reading frame 63	2,5	0,3847
ILMN_23169	10859	LILRB1	leukocyte immunoglobulin-like receptc	2,4	1,0331
ILMN_23764	1438	CSF2RA	colony stimulating factor 2 receptor, al	2,4	0,6097
ILMN_32402	140771	SMCR5	Smith-Magenis syndrome chromosome	2,4	0,3847
ILMN_17306	374860	ANKRD30B	ankyrin repeat domain 30B	2,4	1,0331
ILMN_17784	3606	IL18	interleukin 18 (interferon-gamma-indu	2,4	1,0331
ILMN_22203	285855	RPL7L1	ribosomal protein L7-like 1	2,4	0,7969
ILMN_17367(	226	ALDOA	aldolase A, fructose-bisphosphate	2,4	2,6244
ILMN_21610(	126626	GABPB2	GA binding protein transcription factor	2,4	0,7969
ILMN_24019(	146059	CDAN1	codanin 1	2,4	0,6097
ILMN_22281	221322	C6orf170	chromosome 6 open reading frame 17(	2,4	0,7969
ILMN_18131(	117248	GALNTL2	UDP-N-acetyl-alpha-D-galactosamine:p	2,4	2,6244
ILMN_18155	7766	ZNF223	zinc finger protein 223	2,3	0,3847
ILMN_21016	54799	MBTD1	mbt domain containing 1	2,3	2,6244
ILMN_16914	4826	NNAT	neuronatin	2,3	2,0799
ILMN_21612	57464	FAM40B	family with sequence similarity 40, mer	2,3	0,3847
ILMN_21063	9966	TNFSF15	tumor necrosis factor (ligand) superfan	2,3	1,5007
ILMN_21522	6752	SSTR2	somatostatin receptor 2	2,3	1,2499
ILMN_22732	57835	SLC4A5	solute carrier family 4, sodium bicarbor	2,3	0,3847
ILMN_24047	6817	SULT1A1	sulfotransferase family, cytosolic, 1A, p	2,3	0,0000
ILMN_18039	286451	YIPF6	Yip1 domain family, member 6	2,3	1,2499
ILMN_32601	401082	FLJ25363	uncharacterized LOC401082	2,3	0,7969
ILMN_20937	79862	ZNF669	zinc finger protein 669	2,3	0,3847
ILMN_16534	84839	RAXL1	retina and anterior neural fold homeob	2,2	0,3847
ILMN_17451	23543	RBM9	RNA binding protein, fox-1 homolog (C	2,2	1,5007
ILMN_17601	64121	RRAGC	Ras-related GTP binding C	2,2	1,2499
ILMN_22249(	201895	C4orf34	chromosome 4 open reading frame 34	2,2	1,8141
ILMN_22099	440503	PLIN5	perilipin 5	2,2	0,3847
ILMN_17384	55142	CEP27	HAUS augmin-like complex, subunit 2	2,2	0,7969
ILMN_20974	27071	DAPP1	dual adaptor of phosphotyrosine and 3	2,2	0,6097
ILMN_21062(	284161	GDPD1	glycerophosphodiester phosphodieste	2,2	1,5007
ILMN_17811	4067	LYN	v-yes-1 Yamaguchi sarcoma viral relate	2,2	1,8141
ILMN_22330	26279	PLA2G2D	phospholipase A2, group IID	2,2	0,3847
ILMN_22615	326	AIRE	autoimmune regulator	2,2	0,7969
ILMN_20933	6617	SNAPC1	small nuclear RNA activating complex,	2,2	1,0331
ILMN_16884	8073	PTP4A2	protein tyrosine phosphatase type IVA,	2,2	0,3847
ILMN_20488	80224	NUBPL	nucleotide binding protein-like	2,1	0,3847
ILMN_16766(	404093	CUEDC1	CUE domain containing 1	2,1	0,7969
ILMN_17673	367	AR	androgen receptor	2,1	1,5007
ILMN_18112	160728	SLC5A8	solute carrier family 5 (iodide transport	2,1	0,3847

ILMN_22841	7360	UGP2	UDP-glucose pyrophosphorylase 2	2,1	2,6244
ILMN_16562	79827	ASAM	CXADR-like membrane protein	2,1	2,0799
ILMN_18140	5256	PHKA2	phosphorylase kinase, alpha 2 (liver)	2,1	0,6097
ILMN_17872	84858	ZNF503	zinc finger protein 503	2,1	2,6244
ILMN_20478	56127	PCDHB9	protocadherin beta 9	2,1	0,3847
ILMN_22465	653399	GSTTP2	glutathione S-transferase theta pseudc	2,1	0,7969
ILMN_20700	152926	PPM1K	protein phosphatase, Mg2+/Mn2+ dep	2,1	1,2499
ILMN_23573	2218	FKTN	fukutin	2,1	0,7969
ILMN_18010	6693	SPN	sialophorin	2,0	2,0799
ILMN_32393	442578	STAG3L3	stromal antigen 3-like 3	2,0	1,5007
ILMN_20969	140469	MYO3B	myosin IIIB	2,0	1,5007
ILMN_16760	22982	DIP2C	DIP2 disco-interacting protein 2 homol	2,0	2,6244
ILMN_18126	196	AHR	aryl hydrocarbon receptor	2,0	0,7969
ILMN_16957	27161	EIF2C2	eukaryotic translation initiation factor	2,0	2,0799
ILMN_32464	3187	HNRNPH1	heterogeneous nuclear ribonucleoprot	2,0	0,7969
ILMN_22970	9747	FAM115A	family with sequence similarity 115, me	2,0	1,5007
ILMN_17561	79157	MFSD11	major facilitator superfamily domain co	2,0	1,2499
ILMN_17267	23112	TNRC6B	trinucleotide repeat containing 6B	2,0	0,3847
ILMN_22609	706	TSPO	translocator protein (18kDa)	2,0	1,8141
ILMN_17551	440275	EIF2AK4	eukaryotic translation initiation factor	2,0	0,3847
ILMN_17463	7813	EVI5	ecotropic viral integration site 5	2,0	1,0331
ILMN_18061	57680	CHD8	chromodomain helicase DNA binding p	2,0	1,2499
ILMN_17975	1845	DUSP3	dual specificity phosphatase 3	2,0	1,8141
ILMN_23219	64421	DCLRE1C	DNA cross-link repair 1C	2,0	0,3847
ILMN_24061	11025	LILRB3	leukocyte immunoglobulin-like receptc	2,0	0,7969
ILMN_22747	80736	SLC44A4	solute carrier family 44, member 4	2,0	1,2499
ILMN_23240	800	CALD1	caldesmon 1	1,9	1,8141
ILMN_16893	9891	NUAK1	NUAK family, SNF1-like kinase, 1	1,9	1,2499
ILMN_17913	442582	STAG3L2	stromal antigen 3-like 2	1,9	1,2499
ILMN_17080	4134	MAP4	microtubule-associated protein 4	1,9	0,3847
ILMN_23522	166824	RASSF6	Ras association (RalGDS/AF-6) domain	1,9	0,7969
ILMN_17770	90338	ZNF160	zinc finger protein 160	1,9	0,3847
ILMN_32392	6085	RNY3	RNA, Ro-associated Y3	1,9	0,6097
ILMN_21482	10081	PDCD7	programmed cell death 7	1,9	1,2499
ILMN_18150	5292	PIM1	pim-1 oncogene	1,9	1,8141
ILMN_17956	8073	PTP4A2	protein tyrosine phosphatase type IVA,	1,9	1,8141
ILMN_17146	27327	TNRC6A	trinucleotide repeat containing 6A	1,9	1,2499
ILMN_21824	79801	SHCBP1	SHC SH2-domain binding protein 1	1,9	1,0331
ILMN_18156	10955	SERINC3	serine incorporator 3	1,9	1,2499
ILMN_32285	84222	TMEM191A	transmembrane protein 191A (pseudo	1,9	0,3847
ILMN_32696	255031	FLJ35390	uncharacterized LOC255031	1,9	0,3847
ILMN_17891	3652	IPP	intracisternal A particle-promoted poly	1,9	0,7969
ILMN_17217	5469	PPARBP	mediator complex subunit 1	1,9	2,0799
ILMN_17590	115509	ZNF689	zinc finger protein 689	1,9	2,6244
ILMN_17220	55156	ARMC1	armadillo repeat containing 1	1,9	2,0799
ILMN_20646	91966	CXorf40A	chromosome X open reading frame 40	1,9	2,0799

ILMN_17536	3202	HOXA5	homeobox A5	1,9	0,3847
ILMN_16904	145438	C14orf82	FRMD6 antisense RNA 1 (non-protein c	1,8	0,3847
ILMN_17523	79939	SLC35E1	solute carrier family 35, member E1	1,8	2,0799
ILMN_16913	6772	STAT1	signal transducer and activator of trans	1,8	2,0799
ILMN_23962	27250	PDCD4	programmed cell death 4 (neoplastic tr	1,8	0,7969
ILMN_23360	55714	ODZ3	odz, odd Oz/ten-m homolog 3 (Drosopl	1,8	2,6244
ILMN_17489	83734	ATG10	autophagy related 10	1,8	1,8141
ILMN_22259	2730	GCLM	glutamate-cysteine ligase, modifier sub	1,8	1,2499
ILMN_17656	10056	FARSLB	phenylalanyl-tRNA synthetase, beta sul	1,8	1,0331
ILMN_23514	50863	NTM	neurotrimin	1,8	1,8141
ILMN_17386	286354	C9orf130	chromosome 9 open reading frame 130	1,8	0,7969
ILMN_23461	79230	ZNF557	zinc finger protein 557	1,8	0,3847
ILMN_32266	11145	PLA2G16	phospholipase A2, group XVI	1,8	2,0799
ILMN_20926	124801	LSM12	LSM12 homolog (S. cerevisiae)	1,8	1,8141
ILMN_17031	57226	LYRM2	LYR motif containing 2	1,8	0,3847
ILMN_17873	65068	ALS2CR14	amyotrophic lateral sclerosis 2 (juvenile	1,8	0,3847
ILMN_18094	10357	HMGB1L1	high mobility group box 1 pseudogene	1,7	2,6244
ILMN_18039	51768	TM7SF3	transmembrane 7 superfamily member	1,7	1,5007
ILMN_22708	54663	WDR74	WD repeat domain 74	1,7	1,0331
ILMN_17026	84617	TUBB6	tubulin, beta 6 class V	1,7	0,7969
ILMN_21572	6718	AKR1D1	aldo-keto reductase family 1, member	1,7	1,8141
ILMN_17978	23512	SUZ12	suppressor of zeste 12 homolog (Drosc	1,7	1,2499
ILMN_16790	81931	ZNF93	zinc finger protein 93	1,7	0,3847
ILMN_21754	54516	MTRF1L	mitochondrial translational release fact	1,7	0,7969
ILMN_23626	8824	CES2	carboxylesterase 2	1,7	0,6097
ILMN_17091	497262	RUNDC2C	RUN domain containing 2C	1,7	0,3847
ILMN_23941	55471	PRO1853	chromosome 2 open reading frame 56	1,7	0,3847
ILMN_16798	51186	WBP5	WW domain binding protein 5	1,7	0,7969
ILMN_22194	79056	PRRG4	proline rich Gla (G-carboxyglutamic aci	1,7	0,7969
ILMN_23705	54739	XAF1	XIAP associated factor 1	1,7	1,5007
ILMN_33067	54502	RBM47	RNA binding motif protein 47	1,7	1,2499
ILMN_18155	3203	HOXA6	homeobox A6	1,7	0,7969
ILMN_23937	10093	ARPC4	actin related protein 2/3 complex, subu	1,7	2,0799
ILMN_16575	91057	CCDC34	coiled-coil domain containing 34	1,7	1,0331
ILMN_24144	5935	RBM3	RNA binding motif (RNP1, RRM) protein	1,7	0,3847
ILMN_21802	9980	DOPEY2	dopey family member 2	1,7	1,8141
ILMN_21882	9140	ATG12	autophagy related 12	1,6	0,7969
ILMN_16615	9729	KIAA0408	KIAA0408	1,6	1,0331
ILMN_23876	1235	CCR6	chemokine (C-C motif) receptor 6	1,6	2,0799
ILMN_33014	729324	LOC729324	hCG1986447	1,6	1,2499
ILMN_24080	1936	EEF1D	eukaryotic translation elongation facto	1,6	2,6244
ILMN_17092	81790	RNF170	ring finger protein 170	1,6	1,5007
ILMN_20583	9475	ROCK2	Rho-associated, coiled-coil containing p	1,6	1,8141
ILMN_16853	374928	ZNF773	zinc finger protein 773	1,6	0,3847
ILMN_22150	23594	ORC6L	origin recognition complex, subunit 6	1,6	1,0331
ILMN_20917	123688	LOC123688	aminoglycoside phosphotransferase do	1,6	1,8141

ILMN_17830(	788	SLC25A20	solute carrier family 25 (carnitine/acylc	1,6	0,3847
ILMN_32453(	344787	ZNF860	zinc finger protein 860	1,6	0,6097
ILMN_17606(	3200	HOXA3	homeobox A3	1,6	2,0799
ILMN_21337(	399967	PATE2	prostate and testis expressed 2	1,6	0,7969
ILMN_23648(	8473	OGT	O-linked N-acetylglucosamine (GlcNAc)	1,6	1,0331
ILMN_17695(	54965	PIGX	phosphatidylinositol glycan anchor bios	1,6	0,3847
ILMN_16853(	25870	SUMF2	sulfatase modifying factor 2	1,6	2,0799
ILMN_23790(	84901	NFATC2IP	nuclear factor of activated T-cells, cyto	1,6	0,3847
ILMN_16833(	6482	ST3GAL1	ST3 beta-galactoside alpha-2,3-sialyltra	1,5	1,5007
ILMN_16851(	311	ANXA11	annexin A11	1,5	0,3847
ILMN_16928(	64718	UNKL	unkempt homolog (Drosophila)-like	1,5	1,5007
ILMN_17312(	57714	RNF213	KIAA1618	1,5	0,6097
ILMN_17716(	6629	SNRPB2	small nuclear ribonucleoprotein polype	1,5	1,8141
ILMN_16997(	372	ARCN1	archain 1	1,5	1,8141
ILMN_23630(	5888	RAD51	RAD51 homolog (S. cerevisiae)	1,5	0,3847
ILMN_23655(	7862	BRPF1	bromodomain and PHD finger containi	1,5	0,3847
ILMN_18029(	51588	PIAS4	protein inhibitor of activated STAT, 4	1,5	0,3847
ILMN_21847(	150274	HSCB	HscB iron-sulfur cluster co-chaperone h	1,5	1,0331
ILMN_16993(	84820	POLR2J4	polymerase (RNA) II (DNA directed) pol	1,5	0,0000
ILMN_16525(	29797	DKFZp434K1	POM121 transmembrane nucleoporin-	1,5	0,7969
ILMN_17398(	54820	NDE1	nudE nuclear distribution E homolog 1	1,5	0,7969
ILMN_33044(	728640	LOC728640	family with sequence similarity 133, me	1,5	0,3847
ILMN_22054(	202134	FAM153B	family with sequence similarity 153, me	1,5	2,0799
ILMN_17676(	25851	TECPR1	tectonin beta-propeller repeat contain	1,5	0,7969
ILMN_17757(	55720	TSR1	TSR1, 20S rRNA accumulation, homolog	1,5	0,7969
ILMN_18119(	27246	ZNF364	ring finger protein 115	1,5	0,7969
ILMN_16988(	51776	ZAK	sterile alpha motif and leucine zipper c	1,5	2,0799
ILMN_18027(	79647	AKIRIN1	akirin 1	1,5	1,8141
ILMN_21304(	10945	KDELR1	KDEL (Lys-Asp-Glu-Leu) endoplasmic re	1,5	1,5007
ILMN_17087(	55766	H2AFJ	H2A histone family, member J	1,5	1,5007
ILMN_17222(	5048	PAFAH1B1	platelet-activating factor acetylhydrola	1,5	2,0799
ILMN_16815(	5770	PTPN1	protein tyrosine phosphatase, non-rece	1,5	1,0331
ILMN_16902(	84054	PCDHB19P	protocadherin beta 19 pseudogene	1,5	0,3847
ILMN_17200(	79618	HMBOX1	homeobox containing 1	1,5	1,2499
ILMN_32377(	55331	ACER3	alkaline ceramidase 3	1,5	0,3847
ILMN_17458(	57238	KIAA0492	KIAA0492 protein	1,5	2,6244
ILMN_16998(	5900	RALGDS	ral guanine nucleotide dissociation stin	1,4	0,7969
ILMN_17728(	55893	ZNF395	zinc finger protein 395	1,4	0,7969
ILMN_17369(	7357	UGCG	UDP-glucose ceramide glucosyltransfer	1,4	2,0799
ILMN_17619(	6430	SFRS5	serine/arginine-rich splicing factor 5	1,4	1,2499
ILMN_16614(	10471	PFDN6	prefoldin subunit 6	1,4	1,0331
ILMN_23944(	283635	FAM177A1	family with sequence similarity 177, me	1,4	2,0799
ILMN_21432(	541578	CXorf40B	chromosome X open reading frame 40l	1,4	2,6244
ILMN_16710(	2591	GALNT3	UDP-N-acetyl-alpha-D-galactosamine:p	1,4	1,8141
ILMN_17149(	1629	DBT	dihydrolipoamide branched chain trans	1,4	1,2499
ILMN_32420(	493869	GPX8	glutathione peroxidase 8 (putative)	1,4	1,0331

ILMN_16982	5935	RBM3	RNA binding motif (RNP1, RRM) protei	1,4	1,2499
ILMN_32386	93556	C3orf50	EGF-like and EMI domain containing 1,	1,4	1,8141
ILMN_21019	3187	HNRPH1	heterogeneous nuclear ribonucleoprot	1,4	0,6097
ILMN_16558	57146	TMEM159	transmembrane protein 159	1,4	2,0799
ILMN_16623	9406	ZRANB2	zinc finger, RAN-binding domain contai	1,4	0,7969
ILMN_20903	81875	ISG20L2	interferon stimulated exonuclease gen	1,4	2,0799
ILMN_17137	25	ABL1	c-abl oncogene 1, non-receptor tyrosin	1,4	2,0799
ILMN_20729	7156	TOP3A	topoisomerase (DNA) III alpha	1,4	1,2499
ILMN_20956	80008	TMEM156	transmembrane protein 156	1,4	0,7969
ILMN_32401	84298	LLPH	LLP homolog, long-term synaptic facilit	1,4	1,2499
ILMN_17984	23254	KIAA1026	kazrin, periplakin interacting protein	1,4	0,7969
ILMN_16808	5965	RECQL	RecQ protein-like (DNA helicase Q1-like	1,4	0,3847
ILMN_17881	5872	RAB13	RAB13, member RAS oncogene family	1,4	1,5007
ILMN_16784	162966	ZNF600	zinc finger protein 600	1,4	0,7969
ILMN_16514	57222	ERGIC1	endoplasmic reticulum-golgi intermedi	1,4	0,3847
ILMN_16563	5523	PPP2R3A	protein phosphatase 2, regulatory subu	1,4	1,5007
ILMN_17817	2079	ERH	enhancer of rudimentary homolog (Dro	1,4	2,6244
ILMN_21972	11128	POLR3A	polymerase (RNA) III (DNA directed) po	1,4	1,5007
ILMN_21234	656	BMP8B	bone morphogenetic protein 8b	1,4	0,3847
ILMN_17628	9931	HELZ	helicase with zinc finger	1,4	2,0799
ILMN_16828	8209	C21orf33	chromosome 21 open reading frame 33	1,4	1,8141
ILMN_17715	6240	RRM1	ribonucleotide reductase M1	1,4	1,5007
ILMN_32290	728310	LOC728310	golgin A6 family-like 7, pseudogene	1,4	0,7969
ILMN_17410	8396	PIP4K2B	phosphatidylinositol-5-phosphate 4-kir	1,4	1,0331
ILMN_22916	117177	RAB3IP	RAB3A interacting protein (rabin3)	1,3	1,2499
ILMN_17624	200895	DHFRL1	dihydrofolate reductase-like 1	1,3	2,6244
ILMN_17340	338328	GPIHBP1	glycosylphosphatidylinositol anchored	1,3	1,2499
ILMN_21034	162967	ZNF320	zinc finger protein 320	1,3	0,3847
ILMN_18041	222068	TMED4	transmembrane emp24 protein transp	1,3	1,5007
ILMN_17748	55591	VEZT	vezatin, adherens junctions transmemb	1,3	0,7969
ILMN_17924	3267	HRB	ArfGAP with FG repeats 1	1,3	1,8141
ILMN_21814	147841	SPC24	SPC24, NDC80 kinetochore complex co	1,3	0,7969
ILMN_16765	10390	CEPT1	choline/ethanolamine phosphotransfe	1,3	0,3847
ILMN_17984	3218	HOXB8	homeobox B8	1,3	2,0799
ILMN_23687	387522	TMEM189-U	TMEM189-UBE2V1 readthrough	1,3	2,0799
ILMN_24012	10144	FAM13A	family with sequence similarity 13, mer	1,3	1,2499
ILMN_16684	10350	ABCA9	ATP-binding cassette, sub-family A (AB	1,3	0,7969
ILMN_17710	2617	GARS	glycyl-tRNA synthetase	1,3	2,6244
ILMN_17780	55066	PDPR	pyruvate dehydrogenase phosphatase	1,3	2,6244
ILMN_32364	339736	AK2P2	adenylate kinase 2 pseudogene 2	1,3	0,7969
ILMN_18057	389677	RBM12B	RNA binding motif protein 12B	1,3	0,7969
ILMN_32396	84839	RAX2	retina and anterior neural fold homeob	1,3	0,7969
ILMN_21471	440348	LOC440348	nuclear pore complex interacting prote	1,3	1,5007
ILMN_17425	55149	PAPD1	mitochondrial poly(A) polymerase	1,3	1,0331
ILMN_20579	51101	FAM164A	zinc finger, C2HC-type containing 1A	1,3	0,3847
ILMN_23680	6942	TCF20	transcription factor 20 (AR1)	1,3	0,7969

ILMN_17566	116115	ZNF526	zinc finger protein 526	1,3	2,6244
ILMN_17910	51535	PPHLN1	periphilin 1	1,3	1,8141
ILMN_17188	3225	HOXC9	homeobox C9	1,3	1,8141
ILMN_17310	29896	TRA2A	transformer 2 alpha homolog (Drosoph	1,3	1,0331
ILMN_24074	10922	FASTK	Fas-activated serine/threonine kinase	1,3	0,3847
ILMN_33081	26834	RNU4-2	RNA, U4 small nuclear 2	1,3	2,6244
ILMN_17140	57563	KLHL8	kelch-like 8 (Drosophila)	1,3	0,7969
ILMN_32386	692205	SNORD89	small nucleolar RNA, C/D box 89	1,3	1,2499
ILMN_17196	9725	TMEM63A	transmembrane protein 63A	1,3	2,0799
ILMN_17534	55095	SAMD4B	sterile alpha motif domain containing 4	1,3	2,6244
ILMN_22596	55904	MLL5	myeloid/lymphoid or mixed-lineage leu	1,3	2,6244
ILMN_17876	166647	GPR125	G protein-coupled receptor 125	1,3	1,0331
ILMN_17481	1642	DDB1	damage-specific DNA binding protein 1	1,3	0,7969
ILMN_16921	2768	GNA12	guanine nucleotide binding protein (G	1,3	2,6244
ILMN_17304	114793	FMNL2	formin-like 2	1,3	2,0799
ILMN_17141	94241	TP53INP1	tumor protein p53 inducible nuclear pr	1,3	0,6097
ILMN_17333	83939	EIF2A	eukaryotic translation initiation factor	1,3	1,5007
ILMN_17577	734	OSGIN2	oxidative stress induced growth inhibit	1,3	2,6244
ILMN_21750	6429	SFRS4	serine/arginine-rich splicing factor 4	1,3	2,6244
ILMN_17247	8780	RIOK3	RIO kinase 3 (yeast)	1,3	0,3847
ILMN_17373	4000	LMNA	lamin A/C	1,3	1,5007
ILMN_17656	10371	SEMA3A	sema domain, immunoglobulin domain	1,2	2,6244
ILMN_23303	128387	TATDN3	TatD DNase domain containing 3	1,2	1,2499
ILMN_17669	54988	ACSM5	acyl-CoA synthetase medium-chain fam	1,2	1,2499
ILMN_16768	9975	NR1D2	nuclear receptor subfamily 1, group D,	1,2	2,0799
ILMN_23228	51535	PPHLN1	periphilin 1	1,2	2,6244
ILMN_16834	10452	TOMM40	translocase of outer mitochondrial mem	1,2	1,5007
ILMN_16914	83752	LONP2	lon peptidase 2, peroxisomal	1,2	1,5007
ILMN_32470	26781	SNORA67	small nucleolar RNA, H/ACA box 67	1,2	2,6244
ILMN_16735	127428	C1orf83	transcription elongation factor A (SII) N	1,2	2,0799
ILMN_17760	165324	UBXN2A	UBX domain protein 2A	1,2	1,2499
ILMN_21184	84293	C10orf58	family with sequence similarity 213, me	1,2	0,3847
ILMN_32419	246721	POLR2J2	polymerase (RNA) II (DNA directed) pol	1,2	1,2499
ILMN_32491	81566	CSRNP2	cysteine-serine-rich nuclear protein 2	1,2	1,5007
ILMN_17927	1613	DAPK3	death-associated protein kinase 3	1,2	2,6244
ILMN_16598	26472	PPP1R14B	protein phosphatase 1, regulatory (inhi	1,2	1,8141
ILMN_17271	284390	ZNF763	zinc finger protein 763	1,2	0,3847
ILMN_22909	9973	CCS	copper chaperone for superoxide dism	1,2	1,0331
ILMN_21898	51077	FCF1	FCF1 small subunit (SSU) processome c	1,2	2,0799
ILMN_17687	81608	FIP1L1	FIP1 like 1 (S. cerevisiae)	1,2	1,2499
ILMN_23121	90338	ZNF160	zinc finger protein 160	1,2	0,3847
ILMN_17102	79750	ZNF385D	zinc finger protein 385D	1,2	0,7969
ILMN_17103	644591	LOC644591	peptidylprolyl isomerase A (cyclophilin	1,2	0,3847
ILMN_16827	8870	IER3	immediate early response 3	1,2	0,7969
ILMN_21499	400511	FLJ45256	uncharacterized LOC400511	1,2	0,3847
ILMN_16905	5533	PPP3CC	protein phosphatase 3, catalytic subun	1,2	1,0331

ILMN_18151	400931	FLJ27365	MIRLET7B host gene (non-protein codi	1,2	1,2499
ILMN_17924	10109	ARPC2	actin related protein 2/3 complex, subu	1,2	2,6244
ILMN_17373	96459	FNIP1	folliculin interacting protein 1	1,2	1,8141
ILMN_17116	6477	SIAH1	siah E3 ubiquitin protein ligase 1	1,2	0,7969
ILMN_16954	5786	PTPRA	protein tyrosine phosphatase, recepto	1,2	1,0331
ILMN_17634	23064	SETX	senataxin	1,2	0,3847
ILMN_17246	29988	SLC2A8	solute carrier family 2 (facilitated gluco	1,2	1,2499
ILMN_22290	10201	NME6	NME/NM23 nucleoside diphosphate ki	1,2	0,3847
ILMN_16633	991	CDC20	cell division cycle 20 homolog (S. cerev	1,2	1,8141
ILMN_17194	4437	MSH3	mutS homolog 3 (E. coli)	1,2	0,3847
ILMN_16559	22936	ELL2	elongation factor, RNA polymerase II, 2	1,2	1,2499
ILMN_17138	201895	C4orf34	chromosome 4 open reading frame 34	1,2	0,3847
ILMN_17756	8672	EIF4G3	eukaryotic translation initiation factor	1,2	1,2499
ILMN_32489	619208	C6orf225	chromosome 6 open reading frame 22	1,2	1,5007
ILMN_17227	9743	RICS	Rho GTPase activating protein 32	1,2	1,5007
ILMN_17726	23405	DICER1	dicer 1, ribonuclease type III	1,2	1,0331
ILMN_18009	5717	PSMD11	proteasome (prosome, macropain) 26S	1,2	0,3847
ILMN_17085	27125	AFF4	AF4/FMR2 family, member 4	1,2	2,0799
ILMN_17755	1540	CYLD	cylindromatosis (turban tumor syndror	1,2	0,7969
ILMN_22156	113457	TUBA3D	tubulin, alpha 3d	1,2	2,0799
ILMN_22835	54463	FAM134B	family with sequence similarity 134, me	1,2	1,5007
ILMN_17284	10565	ARFGEF1	ADP-ribosylation factor guanine nuclec	1,2	0,7969
ILMN_17011	9424	KCNK6	potassium channel, subfamily K, memb	1,2	0,7969
ILMN_17920	55596	ZCCHC8	zinc finger, CCHC domain containing 8	1,2	2,0799
ILMN_16808	10046	MAMLD1	mastermind-like domain containing 1	1,2	0,3847
ILMN_17787	51421	AMOTL2	angiomotin like 2	1,2	0,7969
ILMN_17010	2055	CLN8	ceroid-lipofuscinosis, neuronal 8 (epile	1,2	1,0331
ILMN_20986	3995	FADS3	fatty acid desaturase 3	1,2	2,0799
ILMN_32315	91584	PLXNA4	plexin A4	1,2	0,7969
ILMN_17225	905	CCNT2	cyclin T2	1,1	2,0799
ILMN_21971	55308	DDX19A	DEAD (Asp-Glu-Ala-Asp) box polypeptic	1,1	0,6097
ILMN_16739	2969	GTF2I	general transcription factor IIi	1,1	2,0799
ILMN_16616	401475	SRRM1L	serine/arginine repetitive matrix 1 pseu	1,1	1,5007
ILMN_17431	23215	BAT2D1	proline-rich coiled-coil 2C	1,1	2,0799
ILMN_17912	85369	FAM40A	family with sequence similarity 40, mer	1,1	2,6244
ILMN_17531	65125	WNK1	WNK lysine deficient protein kinase 1	1,1	2,6244
ILMN_17827	90333	ZNF468	zinc finger protein 468	1,1	0,3847
ILMN_17548	81545	FBXO38	F-box protein 38	1,1	1,0331
ILMN_17429	7582	ZNF33B	zinc finger protein 33B	1,1	2,0799
ILMN_17348	4524	MTHFR	methylenetetrahydrofolate reductase (	1,1	1,0331
ILMN_17929	4335	MNT	MAX binding protein	1,1	1,8141
ILMN_17202	9320	TRIP12	thyroid hormone receptor interactor 1	1,1	2,6244
ILMN_16685	11037	STON1	stonin 1	1,1	0,7969
ILMN_17251	6905	TBCE	tubulin folding cofactor E	1,1	1,0331
ILMN_16537	130617	ZFAND2B	zinc finger, AN1-type domain 2B	1,1	1,2499

)